2015-04-01

A Compliant Mechanism-Based Variable-Stiffness Joint

Jacob Marc Robinson
Brigham Young University - Provo

A Compliant Mechanism-Based Variable-Stiffness Joint

Jacob Marc Robinson

A thesis submitted to the faculty of
Brigham Young University
in partial fulfillment of the requirements for the degree of

Master of Science

Mark B. Colton, Chair
Larry L. Howell
Marc D. Killpack

Department of Mechanical Engineering

Brigham Young University

April 2015

ABSTRACT

A Compliant Mechanism-Based Variable-Stiffness Joint

Jacob Marc Robinson
Department of Mechanical Engineering, BYU
Master of Science

A review of current variable-stiffness actuators reveals a need for more simple, cost effective, and lightweight designs that can be easily incorporated into a variety of human-interactive robot platforms. This thesis considers the potential use of compliant mechanisms to improve the performance of variable-stiffness actuators. The advantages and disadvantages of various concepts using compliant mechanisms are outlined, along with ideas for further exploration. A new variable-stiffness actuator that uses a compliant flexure as the elastic element has been modeled, built, and tested. This new design involves a variable stiffness joint that makes use of a novel variable transmission. A prototype has been built and tested to verify agreement with the model which shows a reasonable range of stiffness and good repeatability. Ideas for further exploration are identified.

Keywords: compliant mechanisms, variable stiffness actuator, robotics

ACKNOWLEDGMENTS

I would like to acknowledge Dr. Mark Colton for the many ways in which he helped me towards accomplishing my thesis. He has guided me in the research process, given me valuable feedback that has improved my writing and presenting skills, and has been instrumental in securing funding that has allowed me to complete my research. Thank you, Dr. Colton.

I acknowledge and express gratitude for the assistance provided me from the BYU Mechanical Engineering Department. This includes Miriam Busch for her guidance along the path to graduation, Kevin Cole for his technical knowledge and assistance with testing my prototypes, and Nick Hawkins for his constant attention through the design and building of my prototypes.

I would also like to thank my fellow graduate students of the BYU Robotics and Haptics lab: Dallin Swiss, Jeff Hawks, Brandon Norton, and Sam McDonald. They have been an important source of advice and knowledge as questions arose throughout my research.

Lastly, I would like to acknowledge my wife, Holli Robinson, who has supported my pursuit of a Master's Degree even before I supported myself. It was her constant encouragement that kept me motivated through some of the most monotonous phases of this work. Thank you for always supporting and believing in me.

TABLE OF CONTENTS

LIST OF FIGURES

CHAPTER 1. INTRODUCTION

Traditional robots use motors and rigid links to achieve motion and interact with their environment. Unfortunately, this rigidity makes most robots too dangerous to work with humans, whether in close proximity or in direct contact. If a robot encounters an unexpected object along its trajectory, whether it be a wall or a person, the result can be destructive to both the robot and the obstruction. Two main approaches to overcoming this challenge have been explored: software compliance and intrinsic compliance. In software compliance, sensors recognize collisions or impending collisions and the controller responds in a variety of ways, from shutting down the robot to simulating an elastic response [1]. While new methods and algorithms have helped to make robots safer, the response time is limited by the bandwidth of the controller [2]. Intrinsic compliance attempts to reduce these instantaneous impact forces by introducing an elastic element between the actuator and the load. This intrinsic compliance responds without bandwidth delays when an impact occurs. While this compliance can make a robot safer, it may degrade the performance of the robot in other ways, including its accuracy in position control applications.

In this thesis, current devices that use intrinsic compliance are reviewed, namely variable stiffness actuators (VSAs). The use of compliant mechanisms in VSAs is investigated and new concepts to this approach are described and analyzed. Finally, the design and testing of a new VSA that incorporates a compliant mechanism is described. This chapter gives a background of VSAs, compliant mechanisms, and the state of current VSA devices.

1.1 Background

1.1.1 Variable Stiffness Actuators (VSAs)

Variable stiffness actuators incorporate elastic elements, typically between the actuator and the joint axis, with a stiffness that can be changed programmatically [3]. This adds another de-

gree of freedom (stiffness) to each joint that can be incorporated into the control of the robot and therefore improve the performance in certain applications. An ideal variable-stiffness actuator will increase the safety of a robot while maintaining the robot's performance. To do this, a VSA needs to include:

1. Large stiffness range (ideally a completely rigid state for high precision tasks and a low stiffness for safe interactions)
2. Usable deflection range (be able to absorb energy from impacts)
3. Compact design (be able to fit in a robot joint)
4. Minimal energy consumption to maintain stiffness (ideally, when set to a certain stiffness, the joint will not require actuator effort to maintain that stiffness)
5. A relatively simple design (to increase the ease of manufacture)

Based on the need for improved actuators to improve the safety, cost, and portability of robots, and in response to the deficiencies in current variable-stiffness actuators, the goal of this research is to explore the use of compliant mechanisms in variable-stiffness actuators. Compliant mechanisms may provide benefits in the simplicity, cost, and weight of variable-stiffness actuators.

1.1.2 Compliant Mechanisms and Variable Stiffness

Compliant mechanisms are devices that transfer an input force or displacement to another point through elastic body deformation. These mechanisms are becoming more common because they offer advantages such as increased performance, lower cost, reduced weight, lower part count, improved simplicity, and the ability to miniaturize [4]. From expanding solar arrays [5] to synthetic intervertebral discs [6], compliant mechanisms are changing the way engineers design movable devices. Compliant mechanisms have been explored in a limited sense in robotics [7, 8] and haptic interfaces [9–13]. In this thesis we present considerations that will enable the incorporation of compliant mechanisms into the design of variable-stiffness actuators for robotics applications.

Compliant mechanisms typically rely on large-deflection beam elements, which are difficult to model and analyze. To simplify analysis, compliant mechanisms can be represented by the

pseudo-rigid body model, which models a flexible joint as a cantilever pin joint with a concentrated torsional spring (see Figure 1.1).

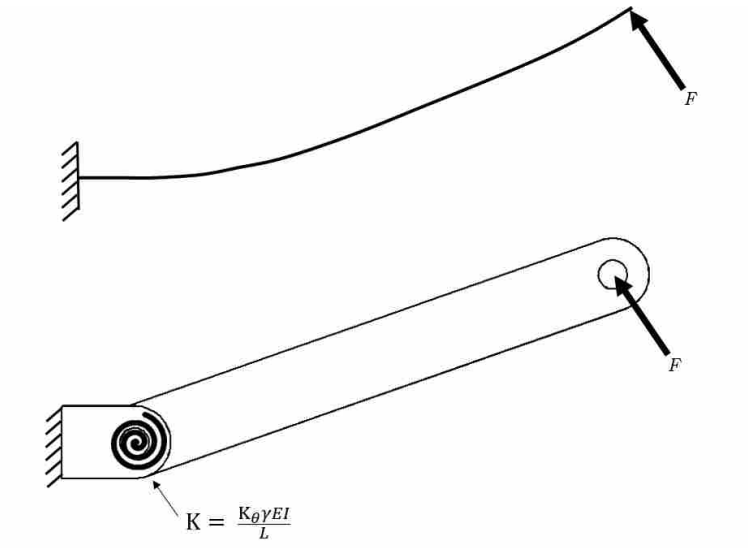

Figure 1.1: The pseudo-rigid body model of a flexible cantilever beam is a cantilever pin joint with a concentrated torsional spring. Alternatively, this model also suggests compliant replacements for typical rotary joints and rigid links.

The stiffness of the "pseudo-rigid body joint" for a cantilever beam can be simplified to

$$K = \frac{K_\theta \gamma EI}{L}, \tag{1.1}$$

where E is the modulus of elasticity, I is the cross-sectional area moment of inertia, L is the length of the beam, and K_θ and γ are constants that depend on the direction of the applied force (F). In addition to serving as a modeling tool, the pseudo-rigid body equivalent suggests compliant replacements for typical rotary joints and rigid links. Figure 1.1 illustrates the replacement of a rigid arm and a rotary joint by a large-deflection cantilever beam.

The reduction of parts and the simplified stiffness analysis make compliant mechanisms potentially advantageous in variable-stiffness actuators. The greatest challenge when using compliant mechanisms in VSAs is achieving a wide range of stiffness while maintaining a usable range of deflection all in a functional size. Increasing the stiffness of a compliant beam generally means

the range of motion of that beam must be reduced to prevent exceeding the stress limits of the beam.

1.2 Literature Review

VSAs can be broadly grouped into antagonistic or serial configurations, depending on the approach to achieving the controllable stiffness. The following is a brief explanation of these two types of VSAs and current devices which employ them.

1.2.1 Antagonistic Configuration

Antagonist configurations generally work in a manner similar to human muscles as shown in the top half of Figure 1.2. The joint angle changes as the two motors move in tandem. As the motors move in opposite directions (antagonistically) the springs are stretched, which pretensions them and the overall joint stiffness increases.

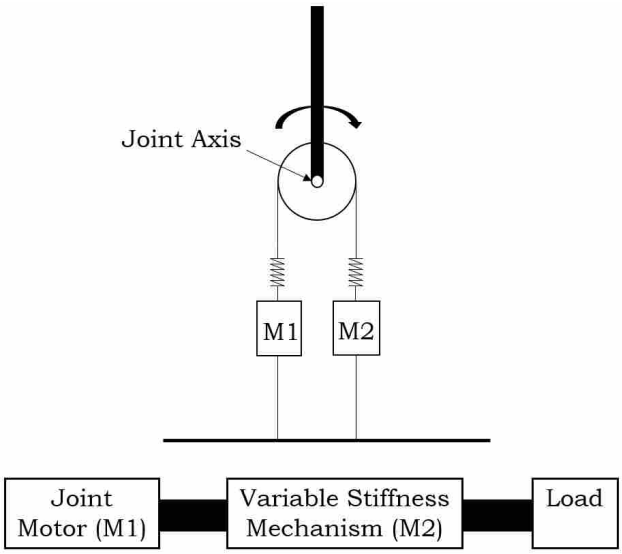

Figure 1.2: Schematic representations of antagonistic (top) and serial (bottom) VSA configurations.

Analysis of current antagonist configurations [14–19] reveals that they fail to meet nearly all of the requirements listed above. For example, [18] developed a biologically inspired antagonistic VSA that is similar to the top half of Figure 1.2, except it uses nonlinear spring mechanisms

in place of the traditional springs. Since the springs must be stretched to increase stiffness, there is a fairly low limit to the maximum stiffness available. Furthermore, as the stiffness increases by deflecting the springs antagonistically, the range of deflection decreases since the springs have already been deflected. This relationship (stiffness to range of deflection) is the key limiting factor for any VSA configuration, however, antagonistic configurations perform very poorly as compared to some serial configurations.

The VSA-CubeBot [14] is an antagonistic VSA that is highly compact and modular. The device employs two hobby style servos in a compact unit with springs set up in a variation of the diagram in Figure 1.2. When a certain level of stiffness is set, the springs are stretched and the device must continue exerting effort to maintain that stiffness. This is inefficient and requires larger actuators to achieve moderate stiffness settings. Another drawback to these devices is that the springs needs to have a nonlinear force-deflection relationship to obtain adaptable compliance [20].

In summary, antagonistic VSAs have small stiffness ranges with a low maximum on that range, have an adverse stiffness-to-range of deflection relationship, and are energy inefficient.

1.2.2 Serial Configuration

In serial configurations, the variable-stiffness element is in series with the joint motor and the load, as illustrated in the bottom half of Figure 1.2. This configuration can also be implemented using a series elastic element with a constant stiffness. These devices are called series elastic actuators and use various control methods to vary the forces felt at the load [20, 21]. Series VSAs can be further classified by how the stiffness is varied:

1. Changing physical properties of the spring – this approach includes changing the elastic modulus, cross sectional area [22], or active length of the spring [23].

2. Changing transmission between load and spring – this approach includes variable transmissions such as changing lever lengths [24, 25] and continuously variable transmissions [26].

Variable-stiffness actuators that employ a serial configuration vary widely in their design and performance. However, analysis of current serial VSA designs shows that the best (as defined by the criteria listed above) applications of the serial configuration use the variable transmission

approach [24–27]. Ideally a variable transmission can produce virtually infinite stiffness ranges while using little to no energy consumption. For example, Figure 1.3 shows the functional diagram of the CompAct-VSA [25] variable stiffness joint that uses a variable transmission. While the stiffness of the physical springs remain constant, the position of the fulcrum changes transmission of force to the springs. As the fulcrum approaches the springs, the overall joint stiffness approaches zero, while at the other end the stiffness approaches infinite. If the fulcrum were actuated using a non-backdrivable mechanism, the actuator would only use energy to change stiffness, not to maintain it.

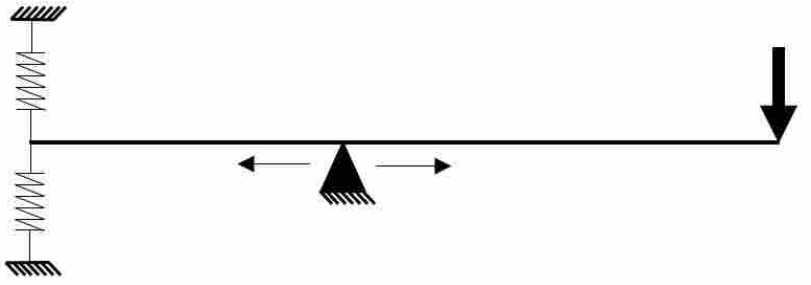

Figure 1.3: A variable-stiffness joint using a variable transmission.

In summary, transmission VSAs exhibit a wide range of stiffness (ideally infinite) while using little energy consumption. The range of deflection is still adversely related to the stiffness, though the relationship can be more explicitly controlled in the design of the mechanism. The major drawback of this approach is that the physical realization of the variable transmission mechanism tends to be complex and costly, such as with the transmission VSA called MESTRAN [26]. This device can achieve an infinite stiffness range while maintaining a good range of deflection, but the mechanism is large and complex with many gears, cams, and sliding parts. Replicating and incorporating a device such as this in a robot would be difficult and costly.

1.3 Motivation

The motivation for this research stemmed from work by the author in robot-assisted autism therapy. A robot named Troy has been built at Brigham Young University to assist therapists in the treatment of children with autism spectrum disorders [28]. Therapists use Troy to engage the

children in interactive and social activities [29] [30]. However, because Troy was constructed using traditional motors and rigid links, the robot is not safe enough to be in close proximity with the children. There is a clear need for a simpler, more modular VSA that could be used to increase the safety of robots such as Troy. With safety as the primary consideration, the present work investigates the benefits of incorporating compliant mechanisms to achieve these goals. While the resultant design must be improved to be used in robots such as Troy, this exploration provides insights into compliant VSA design.

1.4 Contributions

In this research, a new VSA that incorporates a compliant mechanism has been designed, built, and tested. Through the exploration of various compliant VSA concepts and ultimately the design of a new device, the following achievements have been accomplished:

- Identified the strengths and weaknesses of the main approaches to VSA design in the context of safety, modularity, and efficiency
- Identified considerations in the design of compliant mechanism-based VSAs
- Developed a new compliant VSA based on a novel variable transmission mechanism
- Developed and validated a model of the new compliant VSA design

In summary, this research constitutes a more in-depth look into an unexplored area of VSAs: the use of compliant mechanisms. The resultant findings and new device have shown that compliant mechanism are a viable option for VSA designs and may provide significant advantages in reducing complexity while improving performance.

1.5 Thesis Overview

The remainder of this thesis will be organized as follows:

- Chapter 2 describes several concepts that incorporate a compliant mechanism along with analyses of each.

- Chapter 3 describes the design of a new compliant VSA along with a model of the variable joint stiffness.
- Chapter 4 details the experimental setup and results from testing the model described in Chapter 3.
- Chapter 5 includes conclusions about the new compliant VSA design as well as a summary of lessons learned about incorporating compliant mechanisms into VSA design and possible future contributions to this area.

CHAPTER 2. COMPLIANT VARIABLE-STIFFNESS ACTUATOR CONCEPTS

2.1 Introduction

This chapter summarizes a variety of novel approaches explored by the author to incorporate compliant mechanisms into variable-stiffness actuators. The discussion includes strengths and weaknesses of each approach, analyses of key performance criteria, and lessons learned that can inform future compliant mechanism VSA designs.

2.2 Antagonistic (spring pre-load)

As described in the previous chapter, an antagonist configuration uses two actuators. To change joint position the actuators move in tandem and to change stiffness the actuators move in opposite directions and the springs are pre-loaded. One of the major drawbacks of pre-loading the spring is that in order to increase stiffness, the range of deflection must be sacrificed because springs have a limited range of deflection. This is especially true of compliant mechanisms.

One way to create an antagonist VSA using compliant mechanisms is to attach the load (the output link in a robot arm, for example) to two L-shaped flexures. Figure 2.1 shows a conceptual compliant joint (left) with a the pseudo-rigid body equivalent (center and right). The joint is made up of two compliant L-shaped flexures that are fixed together at 1 where the load is applied. 2 and 3 are connected to motors M1 and M2 respectively. 1, 2, and 3 travel through the channel between the rings, thus pivoting about the joint axis, and the rings are fixed to ground. In the pseudo-rigid body equivalent, torsional springs are present at each pin joint. Figure 2.2 illustrates the function of the joint. When a load is applied at 1, the input is deflected with a restoring torque dependent on the joint stiffness (Figure 2.2a). The joint stiffness is determined by the relative positions of M1 and M2. As M1 and M2 move in opposite directions, the joint stiffness changes (Figure 2.2b), while moving them in the same direction changes the joint position (Figure 2.2c). It is important

to note that the corner of the L-shaped flexures are not constrained to the joint axis and are free to move about in the plane.

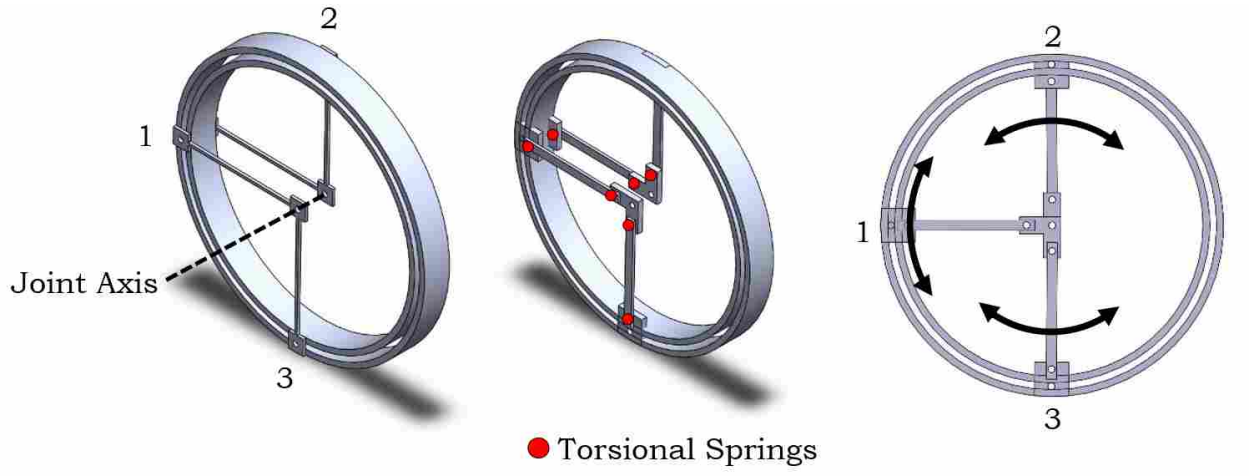

Figure 2.1: Left: Compliant antagonistic VSA conceptual design. The load is attached at 1 to two separate L-shaped flexures that can move independently. Motors M1 and M2 are attached at 2 and 3 to control to stiffness and joint position. Center and right: The pseudo-rigid body model of the compliant VSA. Flexible members are replaced with rigid links, pin joints, and torsional springs at the pin joints.

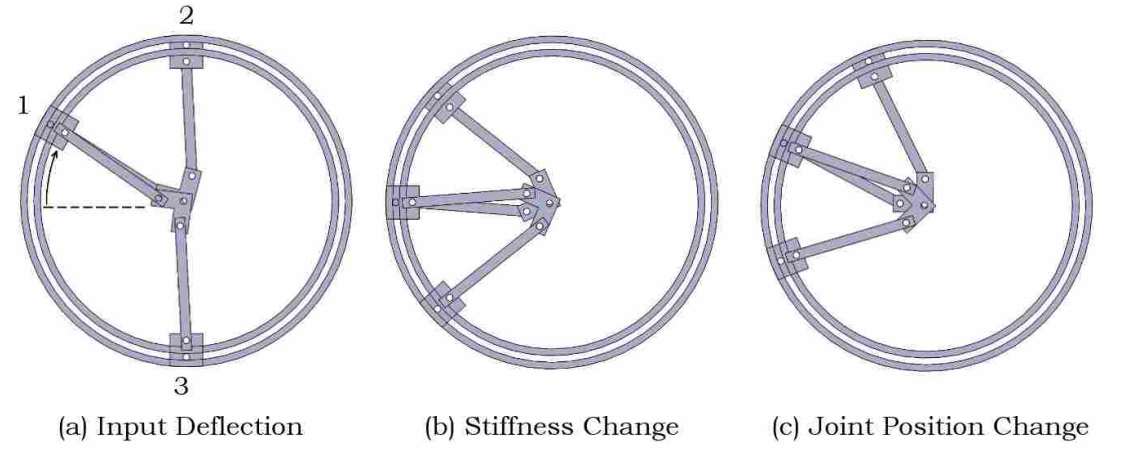

Figure 2.2: Compliant antagonistic VSA functional design. When a load is applied at 1, the input is deflected (a). Changing the position of M1 and M2 in opposite directions changes the joint stiffness (b), while changing M1 and M2 in the same direction changes the joint position (c).

This concept has the benefit of simplicity since the main components for transmitting forces are the springs themselves. These flexures could be easily manufactured, possibly as one piece, and assembled with two hobby servos for M1 and M2. However, this design has some of the same drawbacks as other antagonistic VSAs as outlined below.

1. The minimum and maximum joint stiffness is primarily dependent on the dimensions and material properties of the L-shaped flexures. Since the range of stiffness is relatively small, using flexures with low initial stiffness will allow for a more flexible joint (low minimum stiffness), but the maximum stiffness state would be far from rigid.

2. Increasing the stiffness requires an initial deflection which detracts from the allowed input deflection induced from a load on the joint. This degrades the performance of the mechanism and adds a new mode of failure that could limit the actuator's load capacity.

3. Since the spring-back torque from an input deflection acts on both the input load and the M1 or M2 (depending on the input direction), M1 and M2 torque requirements are directly related to the maximum stiffness. In fact, in a given stiffness setting, such as shown in Figure 2.2b, the spring-back on an input deflection will be the difference between the spring-back torque of both L-shaped flexures. This is because deflecting the input (1) would cause one L-shaped flexure to be deflected more while the other would move toward an undeflected position. This difference means that the torque felt on the input (1) for a given deflection will be less than what M1 or M2 must provide. Thus the joint actuators would need to be over-sized for position control in order to control joint stiffness.

2.3 Changing Physical Properties of the Spring

2.3.1 Additive Concept

One way to change stiffness by changing the physical properties of the spring is to add and remove thin flexible layers to the effective spring (see Figure 2.3). Adding layers effectively increases the cross-sectional area moment of inertia (I) while all other parameters in equation 1.1 remain constant. This has the desired effect of increasing stiffness without increasing stress. The

range and resolution of joint stiffness would be determined by the cross-sectional dimensions of the incremental beams and whether each successive layer was the same as the previous.

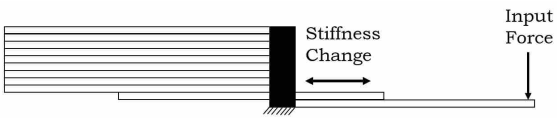

Figure 2.3: A conceptual diagram of adding layers to increase stiffness.

If successive beams maintained the same dimensions and stiffness, then achieving a wide stiffness range with a low minimum stiffness would require many individual flexures. For example, if a stiffness range of 0.1 - 10 Nm/rad were desired, the incremental beam stiffness would be 0.1 Nm/rad. In order to achieve the high stiffness setting, up to 100 flexures would need to be stacked. If successive beams increased in individual stiffness then the device will require fewer layers, but will also exhibit the same adverse stiffness to range of deflection relationship as the previously described approaches. Furthermore, the mechanical complexity of engaging and disengaging this many layers makes this method nearly impossible to construct.

2.3.2 Spring Length

Another way to change the stiffness of a compliant joint is to change the effective length of the compliant beam. Since the pseudo-rigid body stiffness is inversely proportional to the length of the beam, shortening the beam will increase the stiffness (see equation 1.1). However, as stiffness increases so does the stress for a given deflection. To continue increasing stiffness, the range of deflection begins to decrease very quickly. This relationship was examined using a hypothetical open-cross CR joint (OCRJ) with a variable effective length. The OCRJ is a torsional joint that uses four rectangular thin flexures fixed at both ends in a cross formation and rotates about the axis that lies down the middle of the cross [31] (see Figure 2.4). The stiffness of the joint can be varied by changing the effective length of the flexures and is given below [32]. Mounting this variable stiffness joint in series with a traditional actuator would produce a compliant VSA.

The overall joint stiffness is given by [32] as

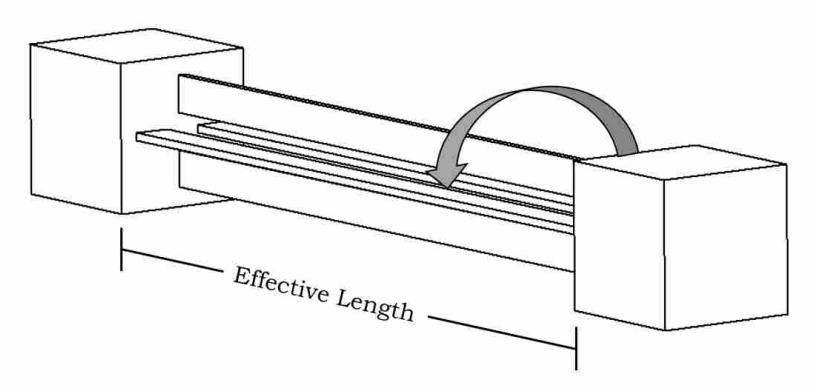

Figure 2.4: Conceptual diagram of the open-cross compliant revolute joint (OCRJ). As the effective length is changed the stiffness of the joint varies.

$$K = \frac{12EI(w+g)^2}{L^3} + \frac{4GK_t}{L} \tag{2.1}$$

where E is Young's modulus, I is the cross-section area moment of inertia, w is the width of the beams, g is the gap between the beams, L is the effective length of the beams, G is the shear modulus, and K_t is the stiffness of the individual beams given by

$$K_t = \frac{wt^3}{16}\left[\frac{16}{3} - 3.36\frac{t}{w}\left(1 - \frac{t^4}{12w^4}\right)\right] \tag{2.2}$$

where t is the thickness of the individual beams. The range of motion of the OCRJ for a given effective length is

$$\text{Range of Motion } (\pm rad) = \frac{0.577\sigma_y L^2 Q}{\left[2.25(EQt)^2(w+g)^2 + 3(K_t GL)^2\right]^{1/2}} \tag{2.3}$$

where σ_y is the yield stress, and Q is defined as

$$Q = \frac{w^2t^2}{3w + 1.8t} \tag{2.4}$$

Figure 2.5 shows the relationship between stiffness and maximum deflection as the effective length of an open cross revolute joint is changed. In this analysis, the OCRJ is comprised of four polypropylene flexures having cross-sectional dimensions of 3.0 x 0.35 mm and a total length of 40 mm. As shown in Figure 2.5, as the effective length is changed, this joint can change from an

infinite stiffness to a moderately low stiffness while maintaining a usable range of deflection, even in the high stiffness settings. For example, with an effective length of 10 mm the joint stiffness is 22.2 Nm/rad and the maximum joint deflection is 12.8 deg. The joint can be brought to an infinite stiffness by bringing the effective length to zero, however, the minimum stiffness setting is limited by the overall joint size which limits the length of the flexures.

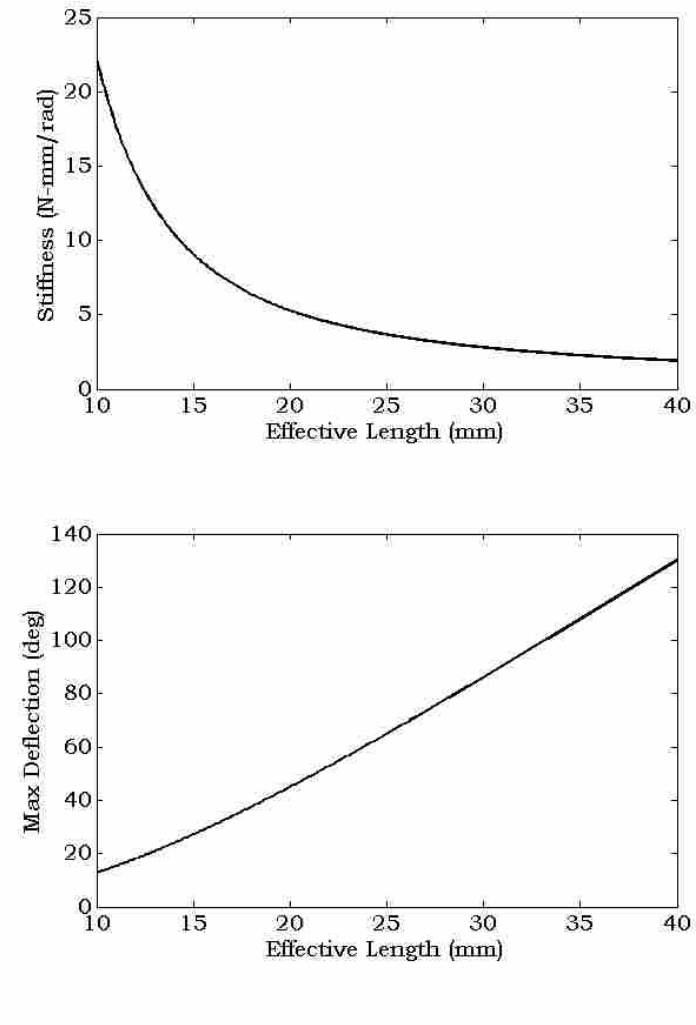

Figure 2.5: The stiffness and maximum deflection ranges for an open-cross CR joint [31] with a variable effective length.

While this design has promising stiffness and deflection ranges, the difficulty lies in constructing the OCRJ with a variable effective length. Changing the length of a compliant beam requires an interface between the beam and the load that is rigid but capable of linear motion

along the beam. This is a challenge for any compliant variable stiffness joint design that utilizes a changing beam length as the method of stiffness adjustment, but is particularly challenging for a torsional member, such as the OCRJ.

One concept that may help alleviate this problem is shown in Figure 2.6, which is a cross-sectional diagram of the flexures and the component that engages them. Instead of engaging the flexures through slits in the fixture, only one side of each flexure would be engaged. To make sure that the spring-back torque is felt in either direction of rotation, half of the flexures would be engaged in one direction of motion, and the other half would be engaged in the other direction. That way tolerance stack-up in manufacturing would not cause any binding or gaps between interfacing parts.

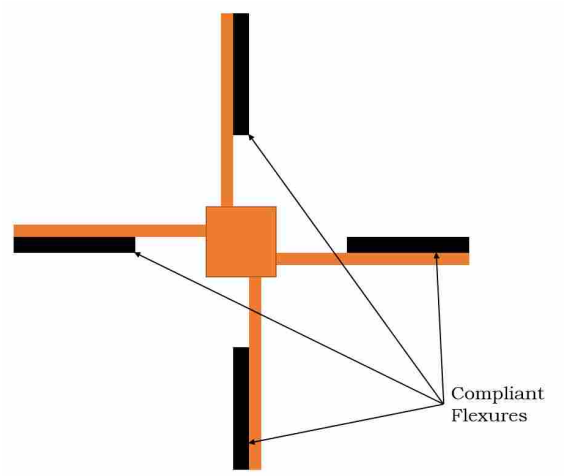

Figure 2.6: Concept of OCRJ cross section showing a way to engage the compliant flexures while avoiding binding issues.

Along with a good stiffness-to-range of deflection relationship, one other possible advantage to the OCRJ is the potential for a compact size. Since the joint uses compliant flexures that are spread out in a radial pattern about the joint axis, it would be possible to overlap the joint motor with the OCRJ along the joint axis. Figure 2.7 shows how the joint motor could be placed inside the compliant flexures that surround it. The VSA will still use a serial approach, with the output shaft of the joint motor attached to the upper link and the input attached to the lower link (such as

a robot arm), but the length of the joint motor can now overlap the length of the OCRJ. This will help reduce the overall size of the VSA.

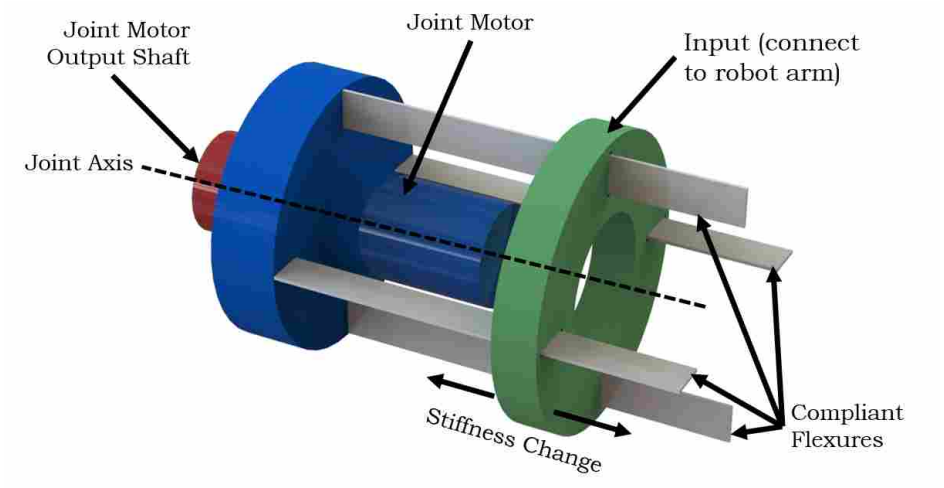

Figure 2.7: OCRJ concept showing how the variable-stiffness joint can be built concentrically outward around the joint motor. Not shown in this schematic is the linear actuator necessary to control the effective length of the beams.

These improvements to the OCRJ may allow for the building and testing of a VSA, based on this variable-stiffness joint, that is more compact and can provide a wider range of stiffness while maintaining a larger range of deflection.

2.4 Changing Transmission Between Load and Spring

Changing the length of a compliant beam can be challenging mechanically, and can also quickly diminish the range of deflection as the stiffness increases. By varying the transmission of deflection from the input link to the compliant beam, the deflection of the compliant beam can be made much less than the deflection of the input link. This allows a wider range of joint deflection. Using a variable transmission provides the possibility of achieving an infinite stiffness range while using minimal energy to control stiffness.

The downside to this approach is that it requires an added mechanism to perform the variable transmission between the load and spring, adding bulk and complexity to the VSA. With traditional springs this includes a mechanism to convert rotational motion of the joint to translation

of the spring. The benefit of using compliant mechanisms is the inherent rotational motion of these mechanisms. This means the only mechanism needed is a variable transmission between the load and the spring. Since current variable-transmission VSAs exhibit wide ranges of stiffness while maintaining good range of motion at minimal energy expense, the use of compliant mechanisms showed a good likelihood of decreasing the size and complexity of these devices while maintaining performance.

Ideally a fully compliant mechanism could be designed which incorporates a transmission and spring in one mechanism. The current work has investigated the design of a variable stiffness compliant joint that uses a compliant flexure attached to a transmission using traditional pins and joints. While not fully compliant, the novel transmission mechanism used in this new variable-stiffness joint is still much simpler in construction than most current variable-transmission VSAs. The design and model of this variable-stiff joint are described in the following chapters.

2.5 Chapter Summary

This chapter was a summary of the various compliant VSA concepts that were investigated, based on traditional and nontraditional VSA approaches. The advantages and disadvantages of each concept were presented. A transmission approach was identified as the most feasible solution to designing a compliant VSA that could meet the requirements listed in Chapter 1. The following chapter is a description of a new compliant VSA that uses a novel transmission to achieve variable stiffness.

CHAPTER 3. A VARIABLE-TRANSMISSION COMPLIANT VSA DESIGN

3.1 Introduction

A new variable-stiffness joint has been designed that uses a flexible beam as the spring connected to a variable-transmission mechanism. Using a variable transmission offers the possibility of a wide range of stiffness while maintaining a usable deflection range and consuming minimal energy for stiffness control. The challenge of this approach is achieving these qualities in a compact mechanism. The mechanism presented in this chapter is simpler than other transmission VSAs that use traditional springs because it uses a compliant beam in connection with a novel variable transmission. This chapter discusses the design and modeling of such a joint. Chapter 4 will then present testing, results, and experimental validation of the model.

3.2 Functional Description

The new variable-stiffness joint employs a variable transmission that changes the ratio between input deflection and deflection of the compliant beam (spring). Since changing the length of a compliant beam quickly diminishes the range of deflection, this device keeps the length of the compliant beam constant. The compliant beam is connected at one end to a rigid lever that is pinned at the point where the characteristic pivot (pseudo-rigid body joint) of the compliant beam is located, as shown in Figure 3.1(a). Since the rigid lever rotates about an axis that is coincident with the characteristic pivot of the compliant beam, the spring-back force from the compliant beam can be represented as a force acting normal to the rigid lever, as shown in Figure 3.1(b).

The input link is the part of the VSA that is connected to the load (such as a robot arm) and can be easily deflected when the VSA is in a "flexible" state. The rigid lever and input link rotate about two different points and are coupled by a variable pivot point (see Figure 3.1(c)). The pivot point can be moved along a line that is collinear with the input link. The variable transmission is

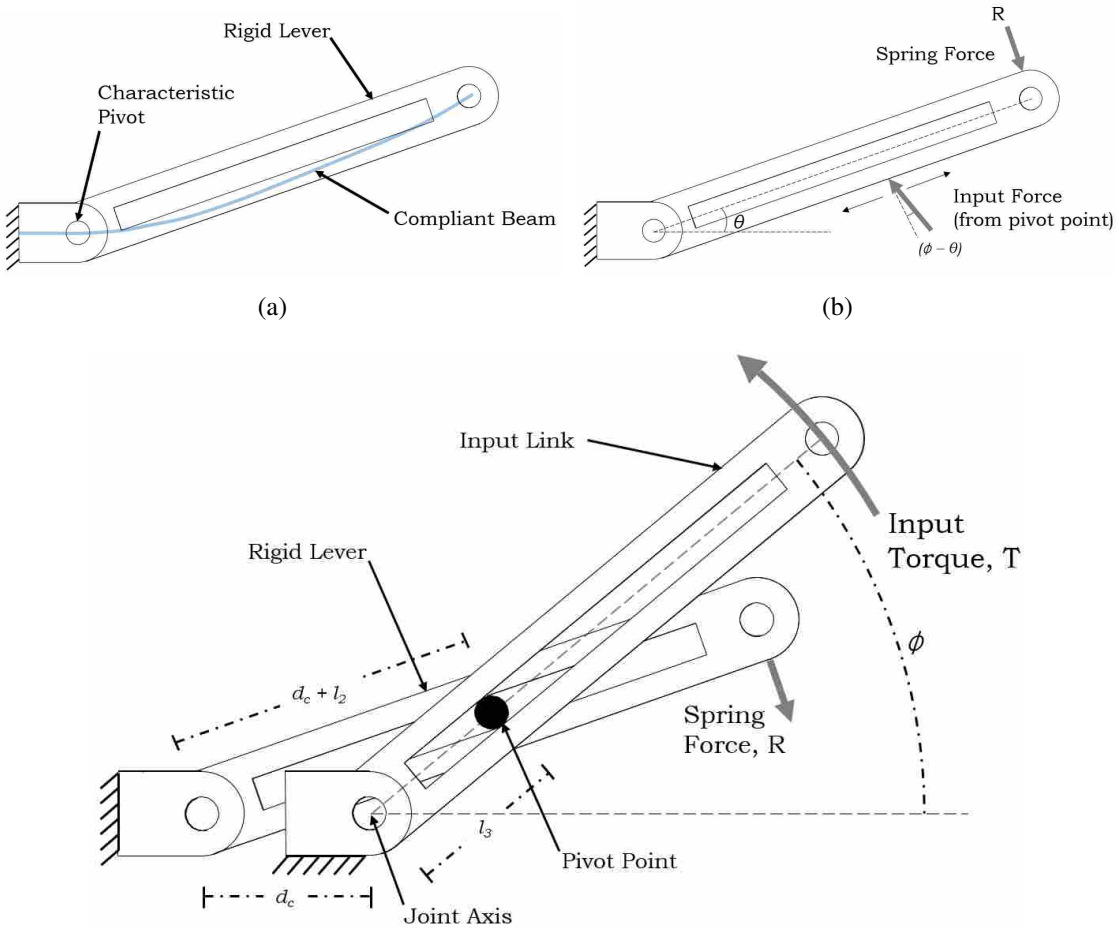

Figure 3.1: A functional diagram of the transmission compliant VSA. The rigid lever is pinned at one end to a compliant flexure which provides a spring-back force as seen in (a) and (b). The input torque applied to the joint (such as a collision) is coupled with the rigid lever through the pivot point (c). Since the input link and rigid lever are pinned at non-concentric centers, deflection of the rigid lever, θ, (and therefore the spring-back force) is dependent on the deflection of the input link, ϕ, and pivot point position, l_2. The position of the pivot point is controlled using a linear servo that is rigidly attached to the rigid lever. This means the pivot point rotates about the rigid lever pivot and l_3 is dependent on the deflection, ϕ.

achieved through changing the position of the pivot point. When the pivot point is aligned with the pivot for the input link, deflecting the input link causes no vertical displacement of the pivot point, and thus no spring deflection. When the pivot point has moved some distance (l_2) away from the input link pivot, the input deflection (ϕ) is transmitted to spring deflection (θ) by

$$\tan(\phi) = \frac{(l_2 + d_c)\sin(\theta)}{(l_2 + d_c)\cos(\theta) - d_c}, \tag{3.1}$$

where l_2 is the distance of the pivot point from the pivot of the input link, and d_c is the distance between the pivots of the rigid lever and the input link. The pivot point is moved using a linear servo that is fixed to the rigid lever and rotates with it. Thus the variable pivot point rotates around the pivot of the rigid lever when an input deflection is introduced. This is explained in Figure 3.1(c) as the distance $(d_c + l_2)$ is constant while the distance l_3 is dependent on the deflection angle (ϕ). When $\phi = 0$, $l_2 = l_3$.

3.3 Variable Stiffness Model

The overall joint stiffness is determined by the distance between pivots (d_c), the dimensions of the compliant beam, and the position of the pivot point (l_2) when $\phi = 0$. These parameters also affect the range of possible deflection, the range of stiffness, and the overall size of the joint. To maximize the range of stiffness while maintaining a smaller form factor, the maximum width and length of the compliant beam were set along with the distance between pivots (d_c). The deflection of the spring was set to a maximum of five degrees and then using stress as the limiting factor, the maximum thickness of the compliant beam was determined to maximize the stiffness of the compliant beam.

From a static analysis, the resulting spring force on the rigid lever can be shown to be

$$R = \frac{K\theta}{\gamma L}, \tag{3.2}$$

Through kinematic analysis, the resultant torque on the input link can be shown to be

$$T = \frac{RL\gamma l_3}{\cos(\phi - \theta)(l_2 + d_c)}, \tag{3.3}$$

where

$$l_3 = \frac{(l_2 + d_c)\sin(\theta)}{\sin(\phi)}. \tag{3.4}$$

Figure 3.2(a) shows that for a given pivot point position (l_2), the predicted torque-displacement relationship is nearly linear. Thus the overall joint stiffness (K_t) is found using a linear fit of the torque-displacement model for a given pivot point position (l_2).

3.4 Variable Stiffness Joint Design

A prototype of the new variable stiffness joint was designed using a compliant beam of 50 mm length and 50 mm width, a distance between pivots (d_c) of 15 mm, and a maximum l_2 of 24 mm. Using polypropylene (E = 1.25 GPa) the maximum thickness of the compliant beam was determined to be 4 mm to achieve a safety factor of 2 with respect to the yield stress of 32.2 MPa. To simplify the construction, the nearest available polypropylene sheet thickness of 3/16 in. (4.76 mm) was used. Using a slightly thicker compliant beam meant that higher joint stiffness would be possible at the expense of range of deflection. Figure 3.2(a) shows the predicted torque-displacement response for various locations of the pivot point (l_2) using the model described by equations (1.1), and (3.1) - (3.4).

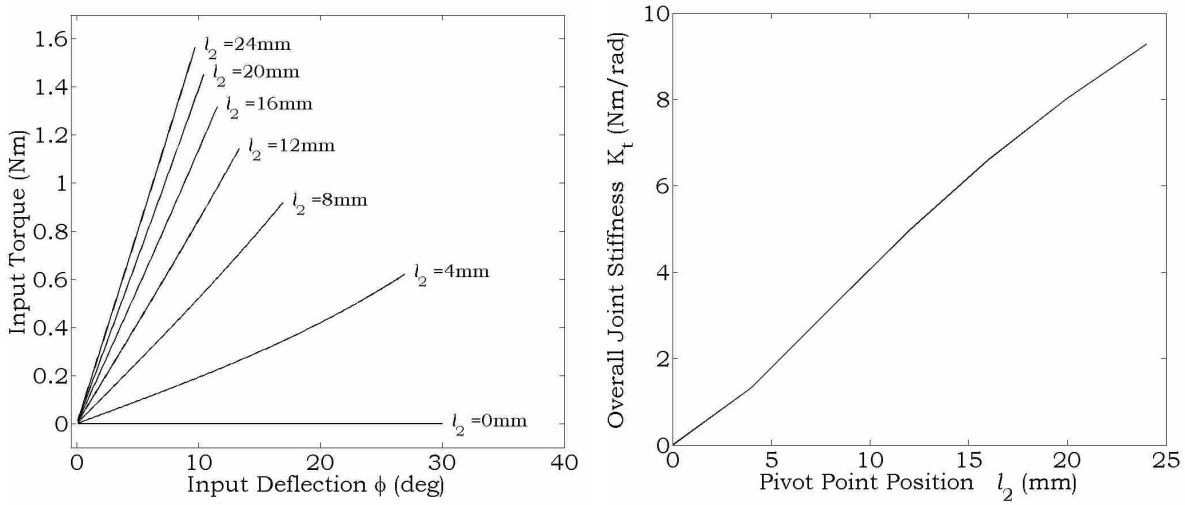

(a) (b)

Figure 3.2: (a) Overall joint input torque and stiffness response over the range of pivot point positions (l_2), (b) Overall joint stiffness over the range of pivot point positions (l_2)

The input deflection (ϕ) is limited to the point where the compliant beam would be at its maximum allowable stress ($S_y/2$), or in other words when θ = 5 deg. The model predicts a range

of stiffness of 0 - 9.28 Nm/rad and at the maximum stiffness setting the maximum input deflection is ϕ = 9.7 deg. As the overall joint stiffness is reduced, the transmission ratio decreases so that a given input deflection, ϕ, results in a smaller spring deflection, θ. Thus decreasing the stiffness equates to decreasing the stress for a given input deflection, ϕ, and the maximum input deflection, ϕ_{max}, is increased. The maximum stiffness could easily be set to infinite by designing a physical stop that would lock the pivot point in place when l_2 was at its maximum distance. However, this prototype does not include this feature and thus the predicted maximum stiffness is 9.28 Nm/rad.

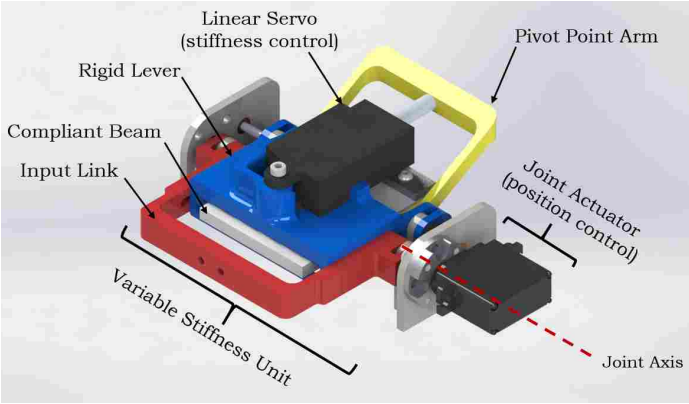

Figure 3.3: CAD representation of the physical prototype for the new variable stiffness actuator.

Figure 3.3 is a CAD representation of the physical prototype that has been built and tested. In this figure the new compliant variable-stiffness joint is attached to a servo motor that would serve as the joint position actuator. As stated, one goal of this design was to make a variable-stiffness joint that could be attached to a variety of joint actuators to allow traditional robots to be easily modified to incorporate variable-stiffness actuators. The new compliant variable-stiffness unit combined with a joint actuator forms a complete variable stiffness actuator, although the current form of the variable-stiffness unit is too large and heavy for practical application.

Figure 3.4 shows how the position of the pivot point changes the deflection of the rigid lever for a given deflection of the input link. As the rigid lever arm is deflected, it also deflects the spring the same amount. Thus changing the pivot point position (l_2) from 6 mm to 22 mm increases the deflection of the spring and therefore the spring back force for the same input joint deflection ϕ.

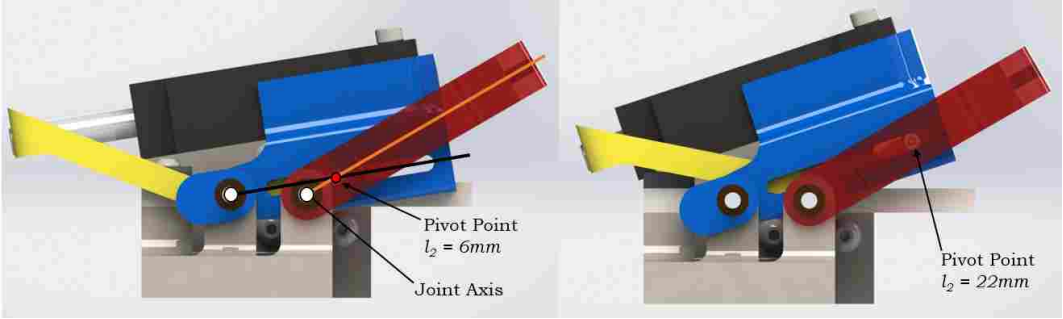

Figure 3.4: Demonstration of how changing the pivot point position (l_2) changes the transmission of the input link (red) deflection (ϕ) to the rigid lever/spring (blue) deflection (θ).

The physical prototype was 3-d printed in polished Alumide (see Figure 3.5). A PoteNit PLS-3050 linear servo was used to control the position of the pivot point. This servo required 12 V to achieve a maximum thrust force of 20 N through a self-contained lead-screw mechanism. Control of the linear servo was accomplished using PWM position control signals from an Arduino microcontroller. In a robot joint context, the robot controller would control the joint angle and stiffness separately. The current design does not include feedback of the joint deflection. Future designs would need to incorporate this feature to achieve closed-loop control of joint position.

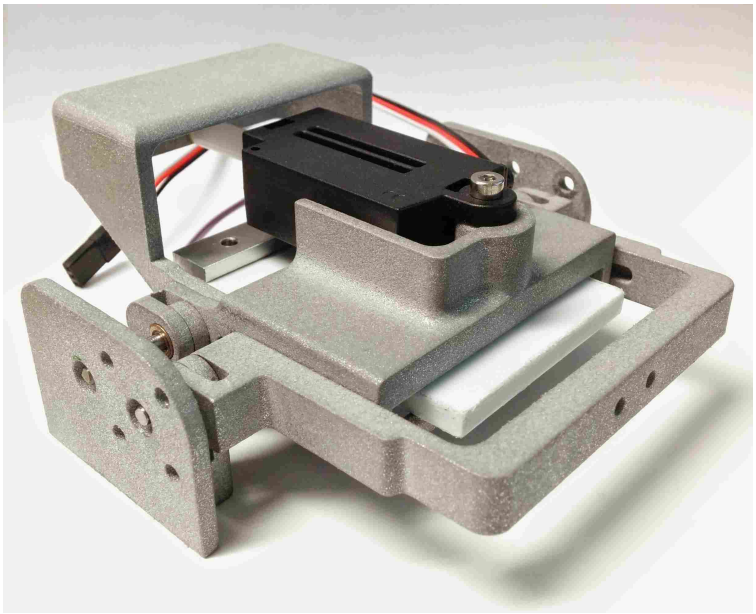

Figure 3.5: Prototype of the new compliant variable-stiffness joint which utilizes a variable transmission mechanism. The main components of the device were 3-d printed in polished Alumide.

3.5 Chapter Summary

This chapter described a new compliant VSA that uses a novel transmission approach. The resultant design is simpler than most other transmission VSAs which is due to the use of a novel "pivot point" transmission coupled with a compliant flexure. A model of the joint stiffness has also been presented. The following chapter explains the methods and results from testing the physical prototype of this mechanism.

CHAPTER 4. TESTING AND VALIDATION

4.1 Introduction

The model described in Chapter 3 was validated by testing the physical prototype on an Instron tensile tester. This chapter describes the testing procedure and results. The results show the device achieves variable stiffness with good repeatability. However, a slight offset in the model compared to the data was also revealed. This discrepancy is explained and accounted for in the model and the resulting calibrated model then matches the data from the Instron testing.

4.2 Experimental Setup

For this new compliant VSA to be used in a robot joint, the stiffness needs to be known at all times. Chapter 3 explained the model used to find stiffness as a function of the pivot point position (l_2). The test described below was performed to check the accuracy of the model against the performance of the physical prototype.

The prototype was mounted in a fixture that allowed the vertical motion of the Instron to apply a torque to the input link, as shown in Figure 4.1(a). This was accomplished by mounting the base of the compliant VSA to the lower grip of the Instron while the input link was pinned to a link that was pinned on its top side to the upper Instron grip. The force gauge made up this connecting link and therefore tensile forces were measured along the direction of this link.

The compliant VSA was tested in seven different stiffness settings with two tests being performed at each setting. The order of the stiffness setting was randomized to avoid any unknown effects of ordering. The stiffness is determined by the location of the pivot point (l_2) which is set using the linear servo. The servo was controlled using an Arduino microcontroller with a button to change the stiffness position. The accuracy of the servo in positioning the pivot point for each run

was verified using a caliper measurement. Tensile force measurements were then recorded as the Instron moved vertically at a rate of 0.01 in/sec.

The measured tensile force and Instron displacement were then translated into angular displacement and applied torque using the known dimensions and kinematics of the fixture. Figure 4.1(b) shows the kinematic chain used in the test fixture. The angle ψ was introduced to find the components of the force gauge measured tensile force (F_m) that cause a torque (T), not shown, on the input link about the joint axis.

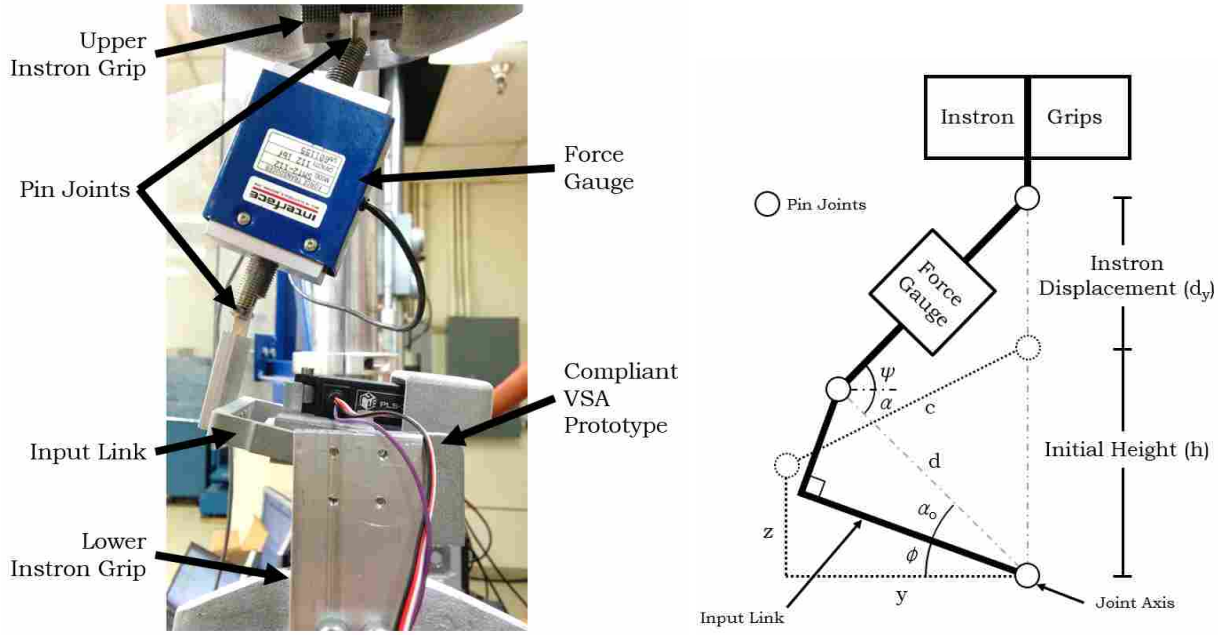

(a) (b)

Figure 4.1: (a) Photo of compliant VSA mounted to Instron for testing. (b) Schematic representation of the kinematic chain used in the Instron fixture. The dotted lines are the undeflected position of the fixture.

The angles ψ and ϕ are functions of the Instron displacement (d_y) and fixture dimensions. To aid in the kinematic analysis, the angles α and α_0 were introduced, where $\phi = \alpha - \alpha_0$. A kinematic analysis of the test fixture yields two independent equations that relate d_y, ψ, and α:

$$h + d_y = c\sin(\psi) + d\sin(\alpha) \tag{4.1}$$

$$d\cos(\alpha) = c\cos(\psi) \tag{4.2}$$

where h, c, and d are constant dimensions of the test fixture. Equations (4.1) and (4.2) can be solved to find α in terms of the Instron displacement (d_y):

$$\alpha = \sin^{-1}\left(\frac{-c^2 + (h+d_y)^2 + d^2}{2d(h+d_y)}\right) \tag{4.3}$$

From equation (4.2), ψ can be found to be

$$\psi = \cos^{-1}\left(\frac{d}{c}\cos(\alpha)\right) \tag{4.4}$$

A static analysis of the fixture shows the torque about the joint axis is

$$T = F_m[\sin\psi(y\cos\phi - z\sin\phi) + \cos\psi(y\sin\phi + z\cos\phi)] \tag{4.5}$$

4.3 Results

From the applied torque calculated in equation (4.5), the model was plotted against the data (see Figure 4.2). The solid lines are the model torque-displacement curves for each stiffness setting, while the test data are shown by the dashed lines.

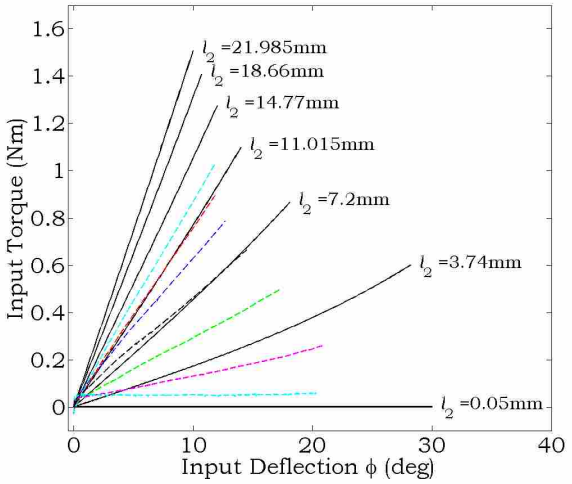

Figure 4.2: Torque-displacement plot of initial model overlaid with test data (dashed lines). There is a discrepancy between the model and data that is likely due to unmodeled flexibility in the components of the variable-transmission.

This figure shows a discrepancy between the model and the test data, suggesting that the prototype was less stiff than predicted. The difference between the model and data is likely due to unforeseen compliance in the device. This is as expected, because unmodeled compliance in series with the modeled compliance can only serve to decrease the overall measured stiffness. Furthermore, variability in the modulus of elasticity may be another source of error. The model was calibrated to the data using a stiffness calibration factor (λ), so that the calibrated modulus of elasticity is $E^* = \lambda E$. After comparing the predicted and actual stiffnesses qualitatively, the value of λ that reduced the discrepancy best was 0.5405.

4.4 Validation

Figure 4.3 shows the results of the Instron test (dashed lines or crosses) overlaid on the calibrated model (solid lines). The results validate the model-predicted stiffness (4.3(b)) for a given pivot point position (l_2), however the nominal torque for a given stiffness and deflection is offset in the prototype due to static friction, as seen at the low deflection range in Figure 4.3(a). This friction offset is dependent on direction of motion, the rate of motion, and the stiffness setting.

The calibrated model now shows that the device is less stiff than originally predicted with a maximum stiffness 5.16 Nm/rad as opposed to 9.28 Nm/rad. Since the prototype is less stiff than expected, it is also capable of more deflection with a maximum deflection of 18 degrees at the maximums stiffness. The prototype in its current state in a robot joint would maintain controllable stiffness, however, the small maximum stiffness may not allow the robot to be precise in dynamic movements. In some circumstances this may be unacceptable. However, in a situation such as autism therapy, where safety is the main concern, this lack of precision may be allowable as long as the maximum stiffness is high enough to achieve adequate motion. The most important consideration may be the ability to achieve a low stiffness state. This would ensure the safety of the robot should a child apply excessive force that would otherwise break the joint components. The new compliant VSA achieves this in a design that is simpler than many other transmission VSAs.

Finally, a qualitative test was performed to verify the performance of the variable-stiffness joint. This was done by mounting the variable-stiffness joint on a hobby servo (HS-322HD) that rotated 90 degrees with an obstruction (a half full bottle) placed in its path. The joint was first set

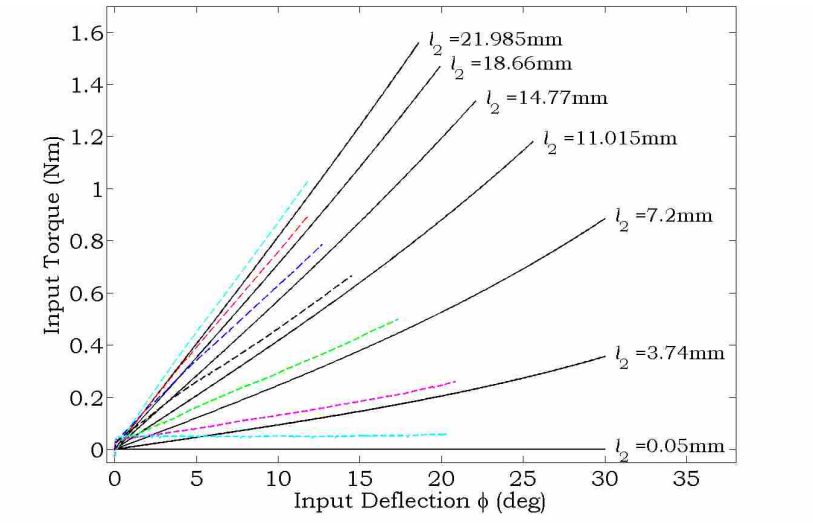

(a)

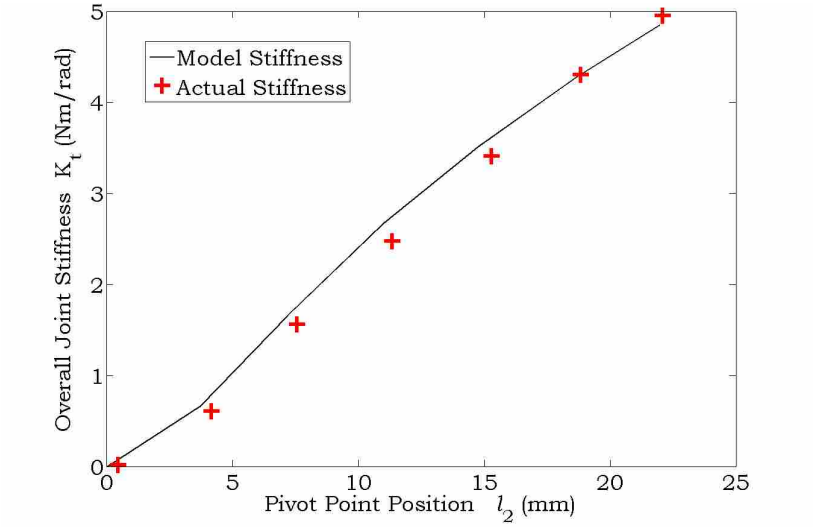

(b)

Figure 4.3: (a) Model-predicted torque (solid lines) versus displacement overlaid with the Instron test results (dashed lines). The offset between the model and data is due to friction in the prototype. (b) Model-predicted stiffness versus pivot point position (l_2) overlaid with the stiffness calculated from the Instron tests.

to a low stiffness with the pivot point at $l_2 = 4mm$. When the robot arm (a blue paddle) came in contact with the bottle, the arm deflected out of the way, not moving the bottle. Then the joint move back to the initial position and changed the stiffness to a higher setting ($l_2 = 20mm$). This time the 90 degree rotation of the servo caused the robot arm to push the bottle over (see Figure 4.4).

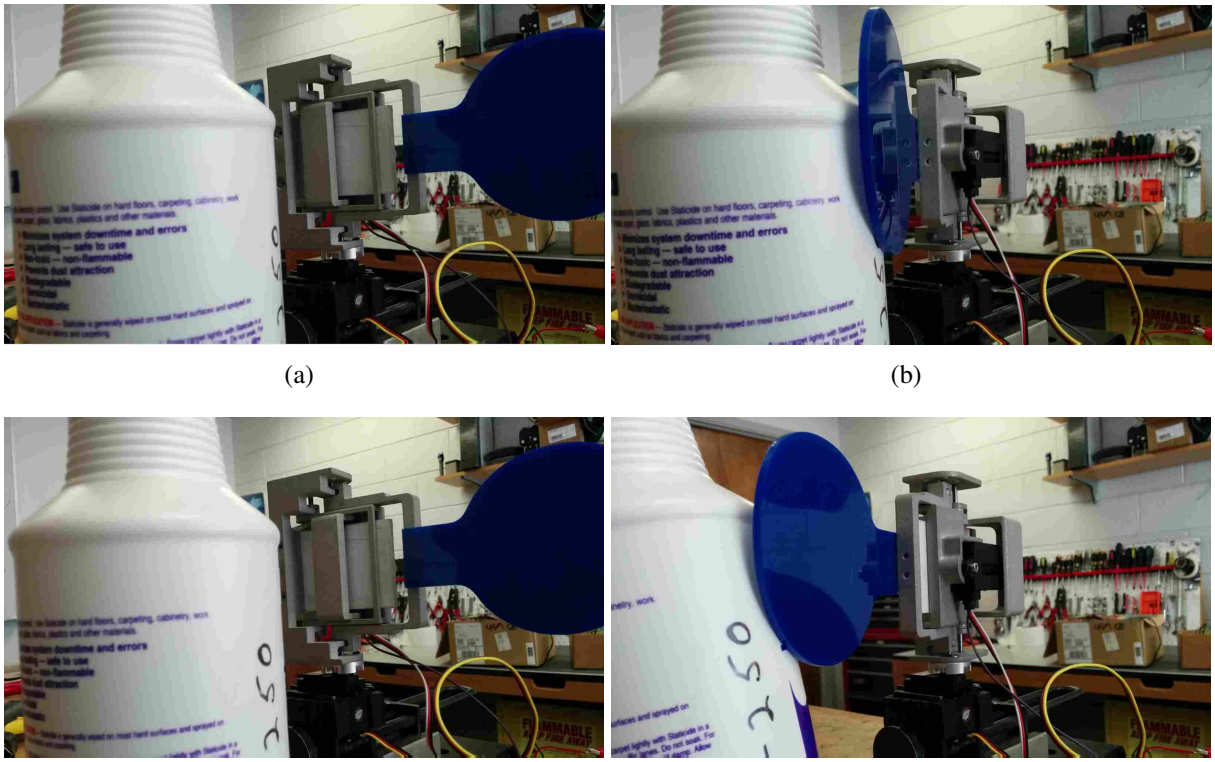

(a) (b)

(c) (d)

Figure 4.4: Images from a demonstration of the variable-stiffness capabilities of the new compliant based VSA. (a) The stiffness is set low ($l_2 = 4mm$). (b) Then the joint servo actuates the joint 90 degrees and the paddle attached to the input link deflects due to a collision with a bottle. (c) The servo returns the joint to zero and the stiffness is increased ($l_2 = 20mm$). (d) The joint is then actuated 90 degrees again and this time the bottle is pushed out of the way of the paddle.

CHAPTER 5. CONCLUSIONS

This research investigated the possibility of using compliant mechanisms in VSA design. From this a detailed summary of current VSA technologies and possible compliant VSA concepts have been presented. A new variable-transmission compliant VSA design has been described along with testing and validation of a physical prototype. This chapter summarizes the accomplishments of this work and presents ideas for future research in compliant VSA design.

5.1 Accomplishments

In this thesis, various compliant VSA concepts have been presented and analyzed with safety and modularity as the key goals. Compliant mechanism-based VSAs have some of the same trade-offs as other VSAs such as an inverse relationship between maximum stiffness and maximum deflection. However, these concepts have shown that compliant mechanisms may provide considerable benefits in the simplicity, cost, and weight of variable-stiffness actuators. While the concepts presented in this paper have their limitations, these approaches to variable-stiffness devices merit further exploration. The following is a summary of the potential for each compliant VSA approach with respect to the design requirements outlined in Chapter 1.

5.1.1 Antagonistic

Large Stiffness Range – In general, an antagonistic approach does not provide a large range of stiffness. This is because increasing the stiffness requires loading the springs, which are limited by the yield stress.

Usable Deflection Range – The yield stress of a spring can be expressed as a maximum deflection. To increase stiffness of the springs, a portion of this limited range must be used. Therefore, increasing the stiffness directly decreases the range of deflection allowed from external deflections (such as collisions).

Compact Design – Antagonistic designs have the potential to be very compact since the variable-stiffness and positioning mechanisms are one and the same. However, higher stiffnesses require larger motors to pretension the springs and resist external deflections.
Minimal Energy Consumption – To maintain a given stiffness setting, the motors must continually exert effort, making antagonistic designs inefficient actuators.
Simple Design – A compliant mechanism-based antagonistic VSA has the potential for simplicity since there is not a necessity for complex mechanisms to achieve transmissions or change beam length.

5.1.2 OCRJ based VSA (changing beam length)

Large Stiffness Range – The OCRJ based VSA is capable of infinitely high stiffness and a low stiffness limit that depends on the design.
Usable Deflection Range – This joint still suffers from a negative relationship between stiffness and range of deflection, however this work has shown that a reasonable range can be designed. For example, in the analysis in Chapter 2 the OCRJ was able to maintain 12.8 degrees of deflection at a stiffness level of 22.2 Nm/rad.
Compact Design – The overall size of this VSA has the potential to be small, but would depend on the specific design. As discussed in chapter 2, the joint motor could possibly be overlapped with the variable-stiffness joint mechanism to decrease the overall size of the VSA.
Minimal Energy Consumption – This joint would act in series with a traditional actuator, which means the stiffness setting only requires energy to change, not to maintain when undeflected. If the stiffness positioning system uses a non-backdrivable mechanism, then there would be no load on the motor even when the joint is deflected.
Simple Design – Simplifying the mechanism for engaging the compliant flexures may prove to be the most difficult challenge for this concept.

5.1.3 Variable-transmission compliant VSA

From this exploration a compliant VSA was designed, modeled, and prototyped to implement a novel transmission variable-stiffness compliant joint in series with a traditional joint

actuator. While this novel design maintains a usable range of deflection for a given stiffness setting, the range of stiffness and overall size of the device needs to be improved. However, this new design illustrates how compliant mechanism can provide much needed benefits to VSAs such as simplification and ease of manufacturing.

Large Stiffness Range – The current design does not have a large range of stiffness, but a new design could adjust the dimensions and material of the spring to achieve a higher maximum stiffness.

Usable Deflection Range – The calibrated model shows a maximum range of deflection at the maximum stiffness setting to be 18 deg.

Compact Design – The prototype is not compact and the design has a major drawback that makes it difficult to make smaller: it must be in series with the joint motor. Since the joint uses a cantilever compliant flexure that must pivot about the joint axis, there is no way to overlap the variable-stiffness joint with the joint motor.

Minimal Energy Consumption – This design requires no energy to maintain a stiffness setting as long as the joint is undeflected. If the joint is deflected, the linear servo still need only exert minimum effort since it uses a lead screw mechanism to transmit linear motion.

Simple Design – When compared to other variable-transmission based VSA devices, the novel transmission mechanism presented in Chapter 4 is much simpler. The simplicity of this design is perhaps the greatest strength of this concept. Further simplification can still be made in moving to a fully compliant structure.

5.2 Future Work

This work has opened the door for further investigation into the various compliant VSA approaches discussed herein. New compliant mechanism-based VSA concepts that use antagonistic and serial variable-stiffness mechanisms may perform better than those presented here.

With regards to the variable-transmission VSA presented in this thesis, future work will investigate a redesign of the prototype to address the deficiencies discussed above and make construction simpler and more compact. This may include a fully compliant structure that uses compliant joints instead of pin joint pivots which can be 3-d printed or injection molded with fewer parts. New prototypes will eliminate the unknown compliance in the structure and allow the model to be correct without calibration. This will make for a more robust model that can be used to investigate

the effects of changing material properties and dimensions of the compliant flexure. Future work will also focus on the integration of this new compliant VSA into interactive robots and examine the safety benefits of such a device.

This thesis has shown that compliant mechanisms offer advantages that may lead to VSAs that are simpler, more compact, and more modular. Further work in this area may lead to the a new VSA that is easier to incorporate into robots such as Troy to increase safety and thereby allow the robot to be more interactive.

REFERENCES

[1] Albu-Schaffer, A., and Hirzinger, G., 2002. "Cartesian impedance control techniques for torque controlled light-weight robots." In *IEEE Int. Conf. Robot. Autom.*, Vol. 1. 1

[2] Haddadin, S., Albu-sch, A., Luca, A. D., and Hirzinger, G., 2008. "Collision Detection and Reaction : A Contribution to Safe Physical Human-Robot Interaction." In *IEEE/RSJ Int. Conf. Intell. Robot. Syst.*, pp. 22–26. 1

[3] Vanderborght, B., Albu-Schaeffer, A., Bicchi, A., Burdet, E., Caldwell, D., Carloni, R., Catalano, M., Eiberger, O., Friedl, W., Ganesh, G., Garabini, M., Grebenstein, M., Grioli, G., Haddadin, S., Hoppner, H., Jafari, A., Laffranchi, M., Lefeber, D., Petit, F., Stramigioli, S., Tsagarakis, N., Van Damme, M., Van Ham, R., Visser, L., and Wolf, S., 2013. "Variable impedance actuators: A review." *Rob. Auton. Syst.,* **61**(12), Dec., pp. 1601–1614. 1

[4] Howell, L. L., Magleby, S. P., and Olsen, B. M., 2013. *Handbook of Compliant Mechanisms*., 1 ed. John Wiley & Sons, Ltd. 2

[5] Zirbel, S. A., Trease, B. P., Magleby, S. P., and Howell, L. L., 2014. "Deployment Methods for an Origami-Inspired Rigid-Foldable Array." pp. 189–194. 2

[6] Halverson, P. A., Howell, L. L., and Bowden, A. E., 2008. "A Flexural-Based Bi-Axial Contact Aided Compliant Mechanism for Spinal Arthroplasty." In *Mech. Robot. Conf.*, pp. 405–416. 2

[7] Norton, B., 2014. "Articulated Spine for a Robot to Assist Children with Autism." Master thesis, Brigham Young University. 2

[8] Evans, M., and Howell, L. L., 1999. "Constant-Force End-Effector Mechanism." In *Proc. IASTED Int. Conf. Robot. Appl. Pap. No. 304-040*, pp. 205–256. 2

[9] Leishman, L. C., Ricks, D. J., and Colton, M. B., 2010. "Design and Evaluation of Statically Balanced Compliant Mechanisms for Haptic Interfaces." In *ASME 2010 Dyn. Syst. Control Conf. Vol. 1*, pp. 859–866. 2

[10] Leishman, L. C., and Colton, M. B., 2011. "A pseudo-rigid-body model approach for the design of compliant mechanism springs for prescribed force-deflections." In *ASME 2011 Int. Des. Eng. Tech. Conf. Comput. Inf. Eng. Conf.*, ASME, ed. 2

[11] Merriam, E. G., Magleby, S., and Colton, M., 2013. "The Design of a Fully Compliant Statically Balanced Mechanism." In *ASME 2013 Int. Des. Eng. Tech. Conf. Comput. Inf. Eng. Conf.* 2

[12] Hawks, J. C., Colton, M. B., Charles, S. K., and Howell, L. L., 2014. "A Variable-Stiffness Compliant Mechanism for Stiffness-Controlled Haptic Interfaces." PhD thesis, Brigham Young University. 2

[13] Gillespie, R. B., Shin, T., Huang, F., and Trease, B., 2008. "Automated characterization and compensation for a compliant mechanism haptic device." *IEEE/ASME Trans. Mechatronics,* **13**(1), pp. 136–146. 2

[14] Catalano, M. G., Grioli, G., Garabini, M., Bonomo, F., Mancini, M., Tsagarakis, N., and Bicchi, A., 2011. "VSA-CubeBot: A modular variable stiffness platform for multiple degrees of freedom robots." In *IEEE Int. Conf. Robot. Autom.*, Ieee, pp. 5090–5095. 4, 5

[15] Van Ham, R., Vanderborght, B., Van Damme, M., Verrelst, B., and Lefeber, D., 2007. "MACCEPA, the mechanically adjustable compliance and controllable equilibrium position actuator: Design and implementation in a biped robot." *Rob. Auton. Syst.,* **55**(10), Oct., pp. 761–768. 4

[16] Catalano, M. G., Grioli, G., Bonomo, F., Schiavi, R., and Bicchi, A., 2010. "VSA-HD: From the enumeration analysis to the prototypical implementation." In *IEEE/RSJ Int. Conf. Intell. Robot. Syst.*, Ieee, pp. 3676–3681. 4

[17] Eiberger, O., Haddadin, S., Weis, M., Albu-sch, A., and Hirzinger, G., 2010. "On Joint Design with Intrinsic Variable Compliance : Derivation of the DLR QA-Joint." In *IEEE Int. Conf. Robot. Autom.*, pp. 1687–1694. 4

[18] Migliore, S. a., Brown, E. a., and DeWeerth, S. P., 2005. "Biologically Inspired Joint Stiffness Control." In *Robot. Autom. 2005. ICRA 2005. Proc. 2005 IEEE Int. Conf.*, no. April, pp. 4508–4513. 4

[19] Tonietti, G., Schiavi, R., and Bicchi, A., 2005. "Design and Control of a Variable Stiffness Actuator for Safe and Fast Physical Human / Robot Interaction." In *IEEE Int. Conf. Robot. Autom.*, no. April, pp. 1–6. 4

[20] Van Ham, R., Sugar, T. G., Hollander, K. W., and Lefeber, D., 2009. "Review of Actuators with Passive Adjustable Compliance/Controllable Stiffness for Robotic Applications." *IEEE Robot. Autom. Mag.*(September), pp. 81–94. 5

[21] Bigge, B., and Harvey, I. R., 2007. "Programmable springs: Developing actuators with programmable compliance for autonomous robots." *Rob. Auton. Syst.,* **55**(9), Sept., pp. 728–734. 5

[22] Kawamur, S., Yamamoto, T., Ishida, D., Ogata, T., Nakayama, Y., and Sugiy, S., 2002. "Development of Passive Elements with Variable Mechanical Impedance for Wearable Robots." In *IEEE Int. Conf. Robot. Autom.*, no. May, pp. 248–253. 5

[23] Hollander, K., Sugar, T., and Herring, D., 2005. "Adjustable Robotic Tendon Using a 'Jack Spring'." In *9th Int. Conf. Rehabil. Robot. 2005. ICORR 2005.*, Ieee, pp. 113–118. 5

[24] Fumagalli, M., Barrett, E., Stramigioli, S., and Carloni, R., 2012. "The mVSA-UT: A miniaturized differential mechanism for a continuous rotational variable stiffness actuator." In *2012 4th IEEE RAS EMBS Int. Conf. Biomed. Robot. Biomechatronics*, Ieee, pp. 1943–1948. 5, 6

[25] Tsagarakis, N. G., Sardellitti, I., and Caldwell, D. G., 2011. "A new variable stiffness actuator (CompAct-VSA): Design and modelling." In *2011 IEEE/RSJ Int. Conf. Intell. Robot. Syst.*, Ieee, pp. 378–383. 5, 6

[26] Vu Quy, H., Aryananda, L., Sheikh, F. I., Casanova, F., and Pfeifer, R., 2011. "A novel mechanism for varying stiffness via changing transmission angle." In *2011 IEEE Int. Conf. Robot. Autom.*, Ieee, pp. 5076–5081. 5, 6

[27] Cano, D., 2013. "Anthropomorphic Adaptation of a Mechanically-variable, Near-infinite Range-of-stiffness Mechanism." PhD thesis, Colorado School of Mines. 6

[28] Ricks, D. J., Colton, M. B., and Goodrich, M. A., 2010. "Design and Evaluation of a Clinical Upper-Body Humanoid Robot for Autism Therapy." *Proc. 2010 Int. Conf. Appl. Bionics Biomech. Venice, Italy*. 6

[29] Goodrich, M. A., Colton, M. B., Brinton, B., Fujuki, M., Atherton, J. A., and Robinson, L., 2012. "Incorporating a robot into an autism therapy team." *IEEE Intell. Syst.*, pp. 1541–1672. 7

[30] Giullian, N., Ricks, D. J., Atherton, J. A., Colton, M. B., Goodrich, M. A., and Brinton, B., 2010. "Detailed requirements for robots in autism therapy." *2010 IEEE Int. Conf. Syst. Man Cybern.*, Oct., pp. 2595–2602. 7

[31] Trease, B. P., Moon, Y.-M., and Kota, S., 2005. "Design of Large-Displacement Compliant Joints." *J. Mech. Des.,* **127**(July), p. 788. 12, 14

[32] Trease, B., 2004. Flexures Lecture Summary Tech. rep., University of Michigan. 12

APPENDIX A. CAD DRAWINGS OF PHYSICAL PROTOTYPE

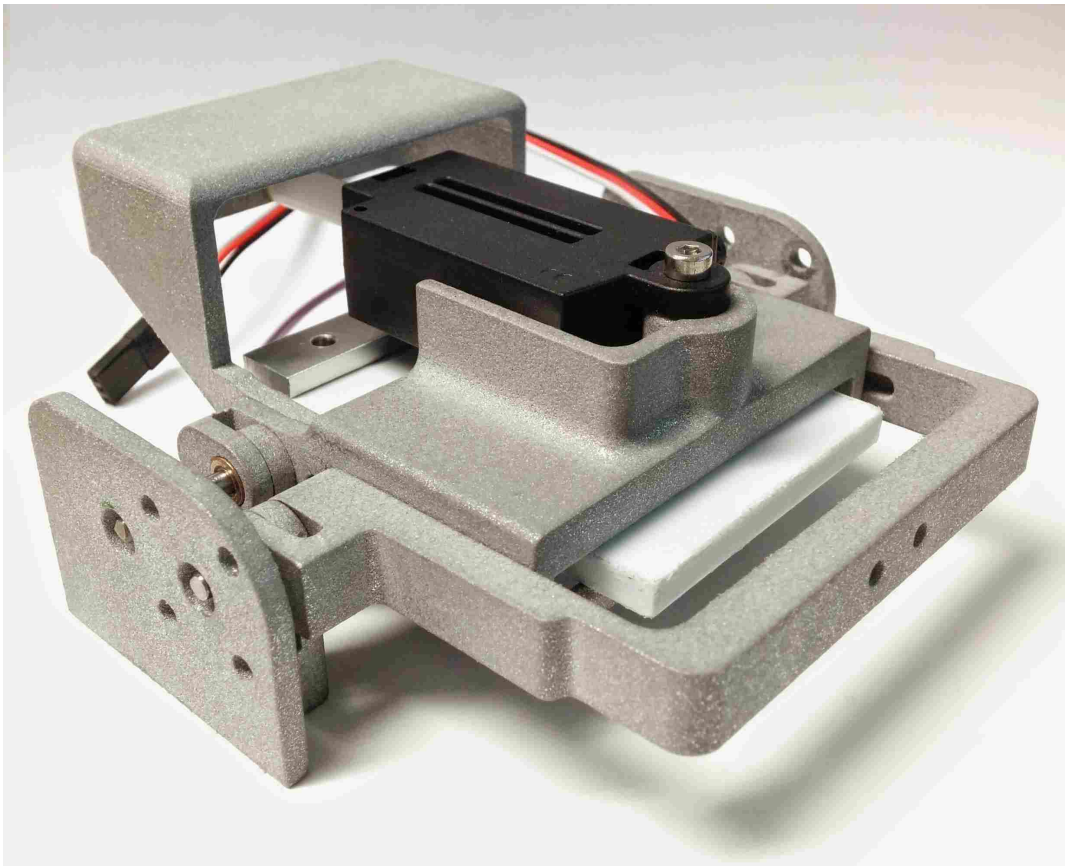

Figure A.1: Physical prototype

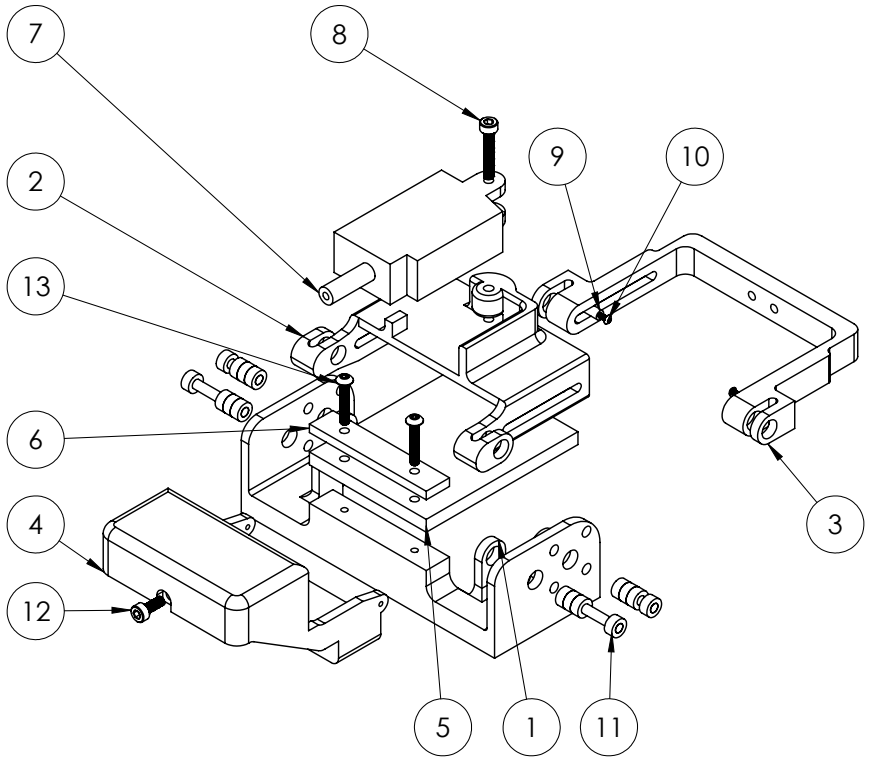

Item No.	PartNo	DESCRIPTION	QTY.
1	3DPARTS-1	BASE	1
2	3DPARTS-2	SPRING LEVER	1
3	3DPARTS-3	INPUT LINK	1
4	3DPARTS-4	PIVOT ARM	1
5	SPRING-1	SPRING	1
6	SPRING-2	SPRING ANCHOR	1
7	PLS-3050	LINEAR SERVO	1
8	91292A029	M3 SS SOCKET HEAD	1
9	91125A142	1/8" OD, STANDOFF	2
10	92949A312	0-80 SS BUTTON HEAD	2
11	9368T95	GRAPHITE BRONZE SLEEVE	16
12	91292A112	M3 SS SOCKET HEAD	1
13	98164A433	4-40 SS BUTTON HEAD	2

NEXT ASSY	USED ON	
APPLICATION		DO NOT SCALE DRAWING

UNLESS OTHERWISE SPECIFIED:

DIMENSIONS ARE IN INCHES
TOLERANCES:
FRACTIONAL ±
ANGULAR: MACH ± BEND ±
TWO PLACE DECIMAL ±
THREE PLACE DECIMAL ±

INTERPRET GEOMETRIC TOLERANCING PER:

MATERIAL

FINISH

	NAME	DATE
DRAWN	JR	3.18.15
CHECKED		
ENG APPR.		
MFG APPR.		
Q.A.		

COMMENTS:

TITLE:

Main ASSY

SIZE	DWG. NO.	REV
A		

SCALE: 1:1.5	WEIGHT:	SHEET 1 OF 1

5 4 3 2 1

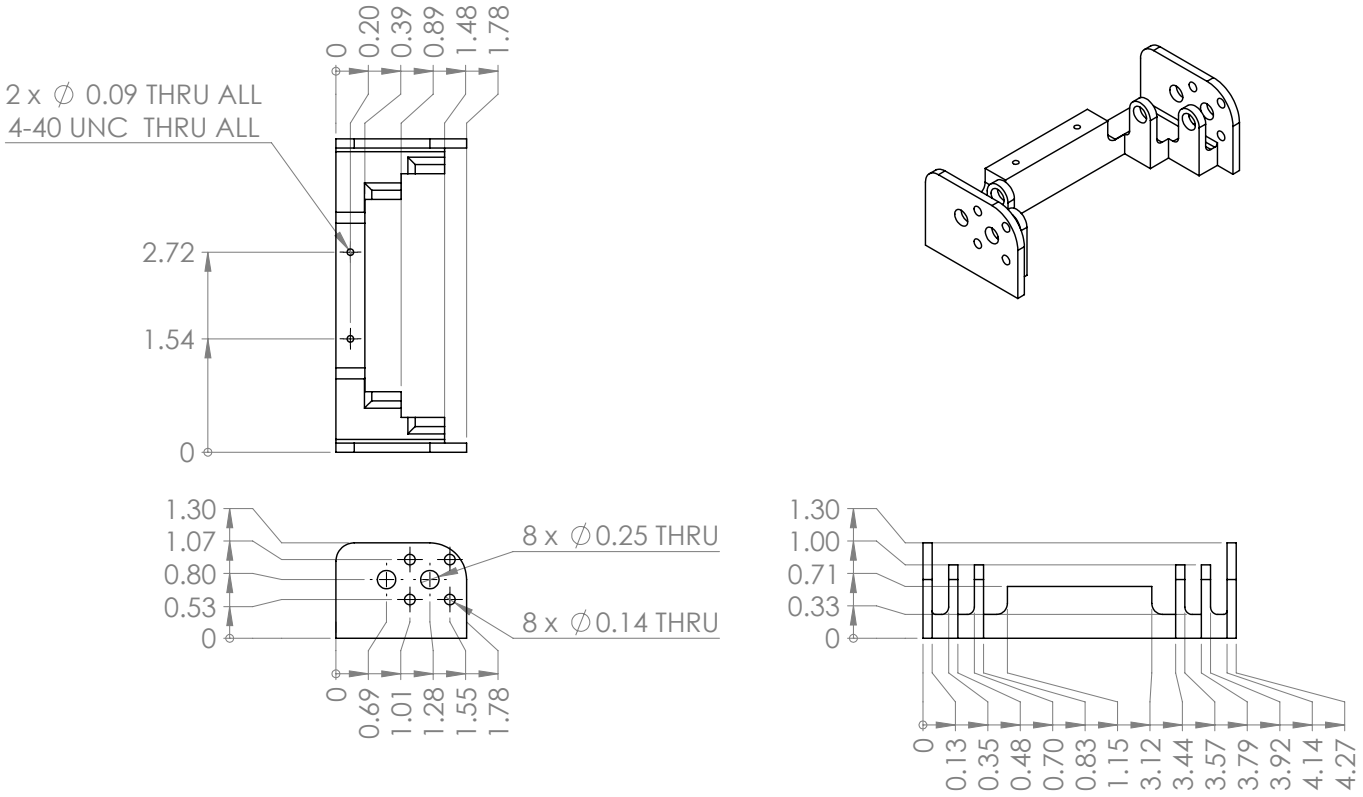

		UNLESS OTHERWISE SPECIFIED:		NAME	DATE
		DIMENSIONS ARE IN INCHES TOLERANCES: FRACTIONAL ± ANGULAR: MACH ± BEND ± TWO PLACE DECIMAL ± THREE PLACE DECIMAL ±	DRAWN	JR	3.18.15
			CHECKED		
			ENG APPR.		
			MFG APPR.		
		INTERPRET GEOMETRIC TOLERANCING PER:	Q.A.		
		MATERIAL	COMMENTS:		
NEXT ASSY	USED ON	FINISH			
APPLICATION		DO NOT SCALE DRAWING			

TITLE:

BASE

SIZE	DWG. NO.	REV
A	1	

SCALE: 1:2	WEIGHT:	SHEET 1 OF 1

5 4 3 2 1

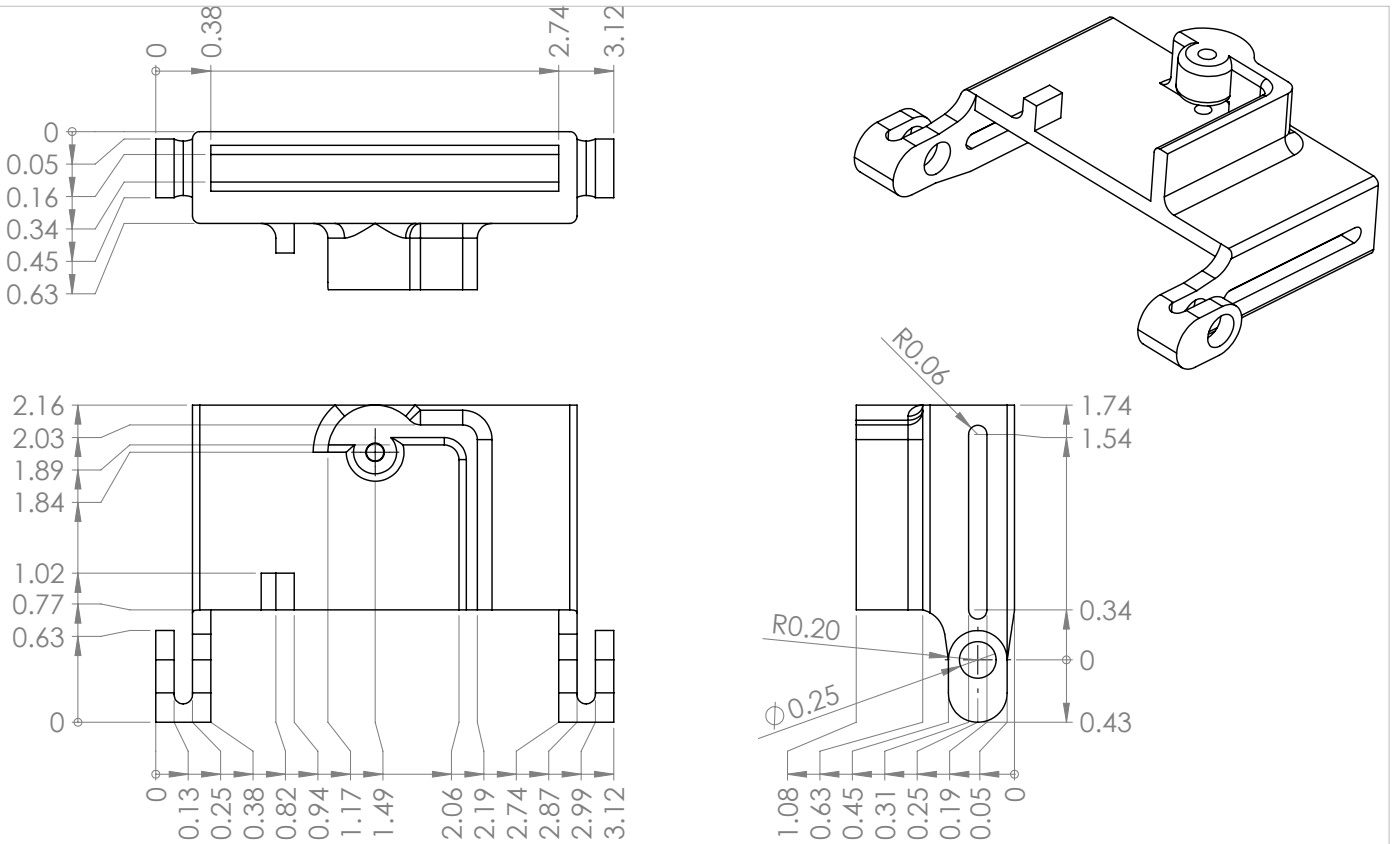

		UNLESS OTHERWISE SPECIFIED:		NAME	DATE
		DIMENSIONS ARE IN INCHES TOLERANCES: FRACTIONAL ± ANGULAR: MACH ± BEND ± TWO PLACE DECIMAL ± THREE PLACE DECIMAL ±	DRAWN	JR	3.18.15
			CHECKED		
			ENG APPR.		
			MFG APPR.		
		INTERPRET GEOMETRIC TOLERANCING PER:	Q.A.		
		MATERIAL	COMMENTS:		
NEXT ASSY	USED ON	FINISH			
APPLICATION		DO NOT SCALE DRAWING			

TITLE:

SPRING LEVER

SIZE	DWG. NO.	REV
A	2	

SCALE: 1:1	WEIGHT:	SHEET 1 OF 1

5 4 3 2 1

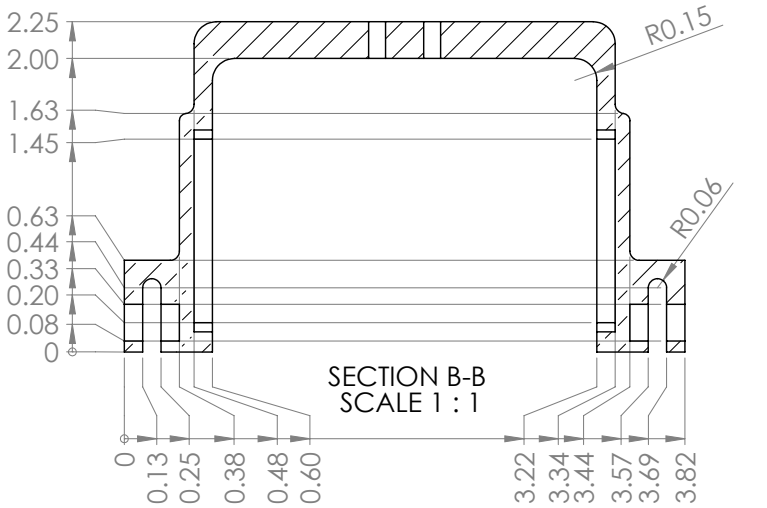

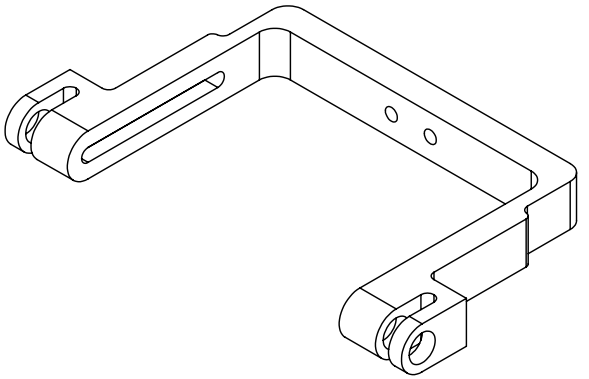

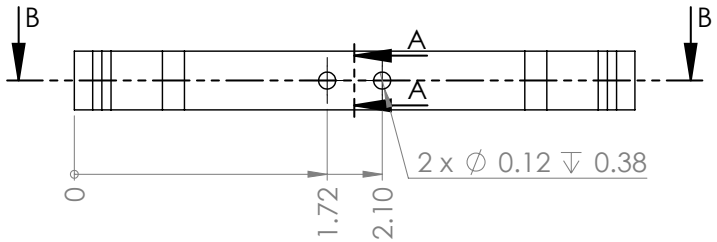

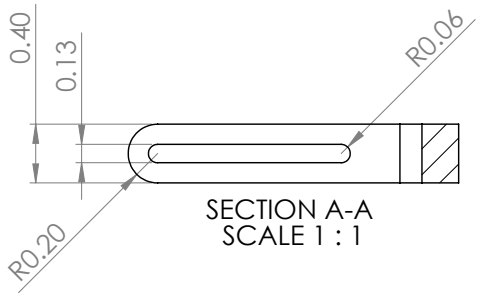

		UNLESS OTHERWISE SPECIFIED:		NAME	DATE
		DIMENSIONS ARE IN INCHES TOLERANCES: FRACTIONAL ± ANGULAR: MACH ± BEND ± TWO PLACE DECIMAL ± THREE PLACE DECIMAL ±	DRAWN	JR	3.18.15
			CHECKED		
			ENG APPR.		
			MFG APPR.		
		INTERPRET GEOMETRIC TOLERANCING PER:	Q.A.		
		MATERIAL	COMMENTS:		
NEXT ASSY	USED ON	FINISH			
APPLICATION		DO NOT SCALE DRAWING			

TITLE:

INPUT LINK

SIZE	DWG. NO.	REV
A	3	
SCALE: 1:1	WEIGHT:	SHEET 1 OF 1

5 4 3 2 1

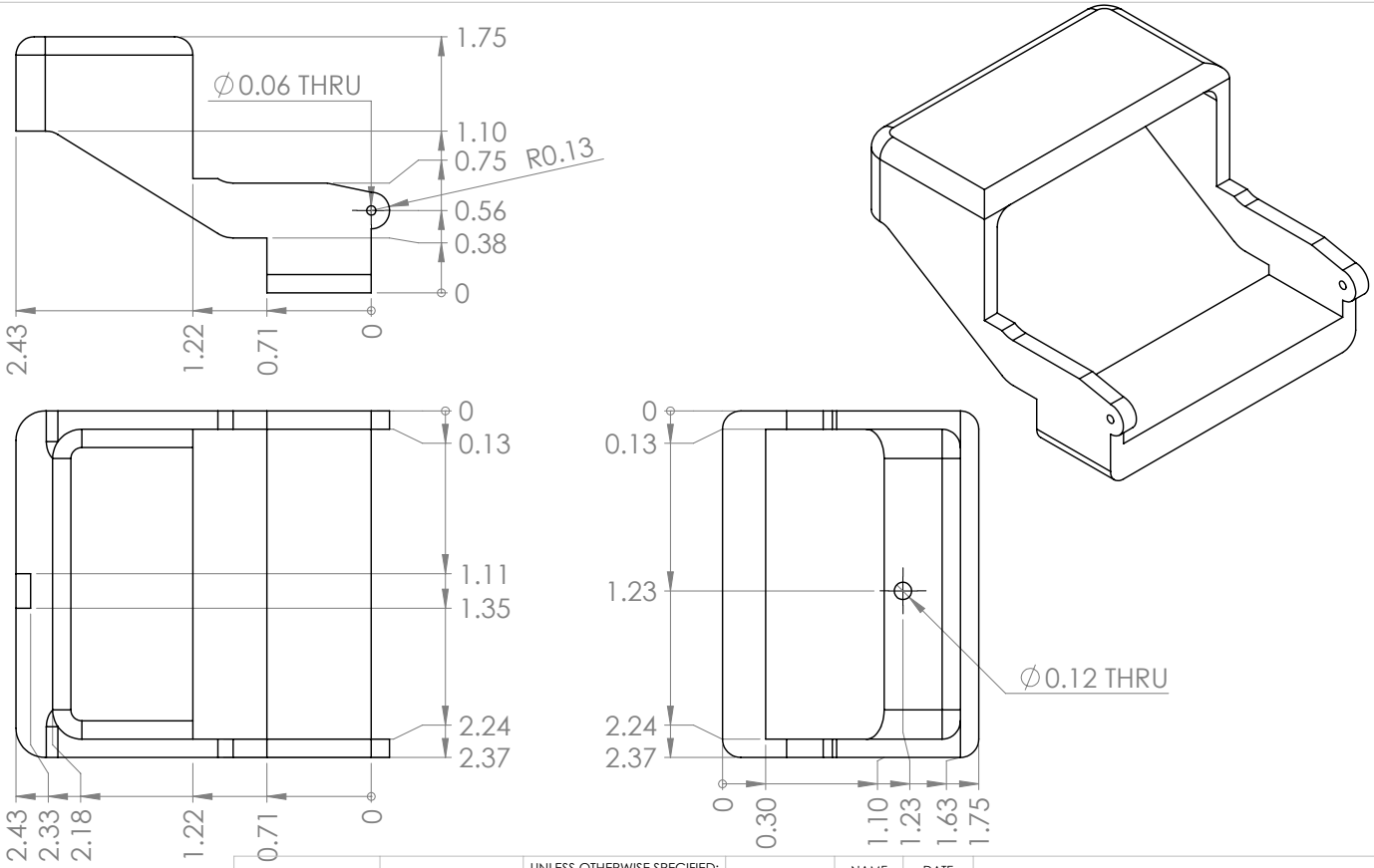

		UNLESS OTHERWISE SPECIFIED:		NAME	DATE
		DIMENSIONS ARE IN INCHES TOLERANCES: FRACTIONAL ± ANGULAR: MACH ± BEND ± TWO PLACE DECIMAL ± THREE PLACE DECIMAL ±	DRAWN	JR	3.18.15
			CHECKED		
			ENG APPR.		
			MFG APPR.		
		INTERPRET GEOMETRIC TOLERANCING PER:	Q.A.		
		MATERIAL	COMMENTS:		
NEXT ASSY	USED ON	FINISH			
APPLICATION		DO NOT SCALE DRAWING			

TITLE:

PIVOT ARM

SIZE	DWG. NO.	REV
A	4	

SCALE: 1:1	WEIGHT:	SHEET 1 OF 1

5 4 3 2 1

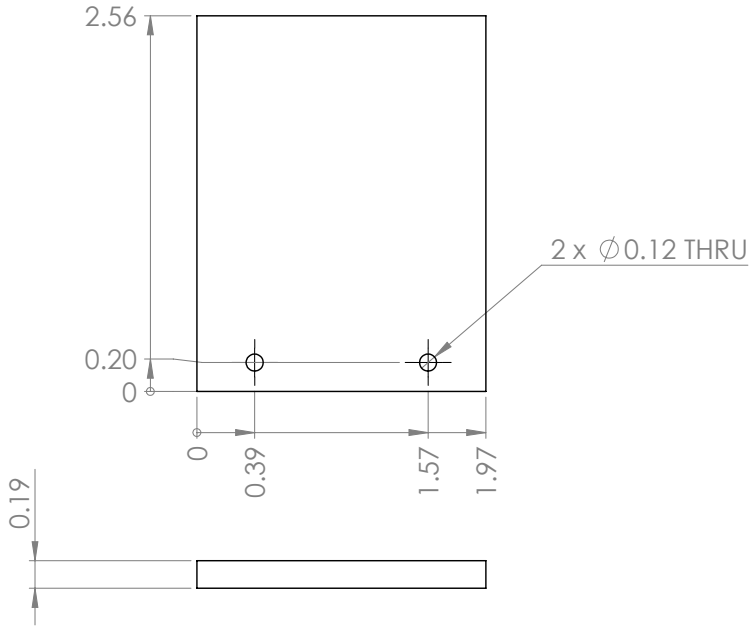

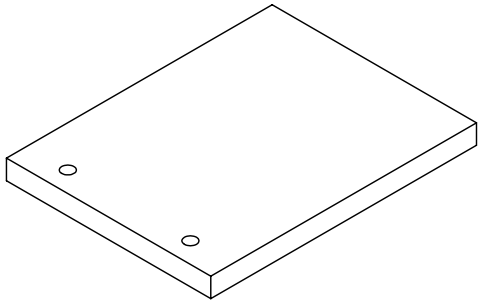

		UNLESS OTHERWISE SPECIFIED:		NAME	DATE
		DIMENSIONS ARE IN INCHES TOLERANCES: FRACTIONAL ± ANGULAR: MACH ± BEND ± TWO PLACE DECIMAL ± THREE PLACE DECIMAL ±	DRAWN	JR	3.18.15
			CHECKED		
			ENG APPR.		
			MFG APPR.		
		INTERPRET GEOMETRIC TOLERANCING PER:	Q.A.		
		MATERIAL	COMMENTS:		
NEXT ASSY	USED ON	FINISH			
APPLICATION		DO NOT SCALE DRAWING			

TITLE:

SPRING

SIZE	DWG. NO.	REV
A	5	
SCALE: 1:1	WEIGHT:	SHEET 1 OF 1

5 4 3 2 1

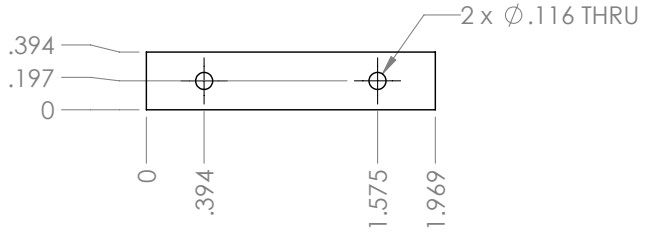

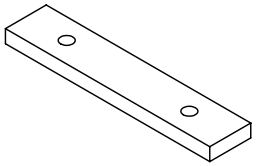

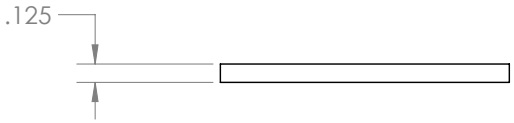

		UNLESS OTHERWISE SPECIFIED:		NAME	DATE
		DIMENSIONS ARE IN INCHES TOLERANCES: FRACTIONAL ± ANGULAR: MACH ± BEND ± TWO PLACE DECIMAL ± THREE PLACE DECIMAL ±	DRAWN	JR	3.18.15
			CHECKED		
			ENG APPR.		
			MFG APPR.		
		INTERPRET GEOMETRIC TOLERANCING PER:	Q.A.		
		MATERIAL	COMMENTS:		
NEXT ASSY	USED ON	FINISH			
APPLICATION		DO NOT SCALE DRAWING			

TITLE:

Spring Anchor

SIZE	DWG. NO.	REV
A	6	
SCALE: 1:1	WEIGHT:	SHEET 1 OF 1

5 4 3 2 1